1-1-1962

Simultaneous development of velocity and temperature profiles for laminar flow of a non-Newtonian fluid in the entrance region of flat ducts.

Joseph Y. Yau
University of Windsor

SIMULTANEOUS DEVELOPMENT OF VELOCITY AND TEMPERATURE PROFILES FOR LAMINAR FLOW OF A NON-NEWTONIAN FLUID IN THE ENTRANCE REGION OF FLAT DUCTS

A Thesis
Submitted to the Faculty of graduate Studies through
the Department of Chemical Engineering in Partial
Fulfillment of the Requirements for the Degree
of Master of Applied Science at Assumption
University of Windsor

by

JOSEPH Y. YAU
B.A.Sc., Assumption University of Windsor, 1961

Windsor, Ontario, Canada
1962

APPROVED BY:

ABSTRACT

A theoretical analysis for the laminar non-Newtonian fluid flow in the entrance region of a flat duct is presented in this thesis. The non-Newtonian fluid is assumed to be of the Ostwald-de Waele model and its physical properties are assumed to be constant. The initial velocity and temperature profiles of the fluid prior to its entry are considered to be flat, and the walls of the duct are maintained at uniform but different temperatures. The momentum and energy integral method of von Karman and Pohlhausen is applied for the solution of entrance heat transfer problems. Dimensionless expressions for velocity and temperature profiles, as well as pressure loss and Nusselt's modulus are obtained from numerical methods.

The results of this thesis indicate that, as in the case of Newtonian fluid, the parameters which influence entrance heat transfer are L/D ratio, Reynolds number and Prandtl number, provided these groups are properly defined for non-Newtonian fluids.

ACKNOWLEDGEMENT

The author wishes to express his gratitude to Dr. C. Tien, whose supervision, able direction and continuous help make this thesis possible. Thanks are extended to Steven Nuspl for the assistance in programming for the use of LGP-30 digital computer, and to B.Y. Tam for carrying out part of the numerical calculations. Grateful acknowledgement is also made to the Ontario Research Foundation for the grant in support of this work.

TABLE OF CONTENTS

LIST OF FIGURES

LIST OF TABLES

CHAPTER I

INTRODUCTION

The problem to be considered here is the simultaneous development of velocity and temperature profiles of a non-Newtonian fluid initially at uniform temperature, and with a flat velocity profile entering a flat duct. A constant temperature (but different from the fluid temperature) is imposed on the walls of the duct. Besides its academic interest, the study of this problem has certain practical significance. The model under present investigation is believed to give a closer approximation of a short-tube heat exchanger. Previous work has shown that the development of velocity profile has a profound effect on the heat transfer characteristics (7, 8, 15).

During recent years, considerable research has been developed in the study of non-Newtonian fluids. This is because an increasing number of fluids treated in industry behave differently from the well-established Newtonian theory. Their shear stress (τ_{yx}) is not directly proportional to the velocity gradient ($-du/dy$). They are referred to as non-Newtonian fluids. However, most of the work done in the past deals with the physical and chemical properties of the fluid and the establishment of mathematical models

to descibe its behavior. Further work in the investigation of the flow and heat transfer characteristics of non-Newtonian fluids would be desirable and most helpful to the engineer.

Theoretical analysis and experimental work have been carried out for laminar flow of various non-Newtonain models (2, 6, 12, 19) whose steady-state relation between shear stress and velocity gradient can be represented by empirical equations. The study of velocity development in the entrance region has been reported by Bouge (3), Tomaya (18), and recently by Collins and Schowalter (5). Heat transfer study with fully developed flow has been investigated by Lyche and Bird (11) and Tien (17). However, studies on simultaneous development of velocity and temperature profiles have not yet been published in literature.

Entrance heat transfer studies for Newtonian fluid have been made only recently. Based on the results of Langhaar (10) on velocity profile development, temperature distribution in the entrance region of a pipe was obtained by Kays (8) and Goldberg (7) using different techniques. Similar study for the case of a flat duct was given by Sparrow (15) in which the integral method was employed.

The study of non-Newtonian flow is a branch of the "science of deformation and flow" known as the science of rheology. As implied by their generalized name, non-Newtonian fluids include all gases, liquids, colloidal

suspensions, polymeric solutions, and crystalline materials which do not obey the Newtonian postulate of viscosity that viscosity depends only on temperature and pressure and is independent of the rate of shear. Wilkinson (19) classified the non-Newtonian fluids into three broad types:

(1) time-independent fluids for which the rate of shear at any point is a function of the shearing stress at that point.

(2) time-dependent fluids for which the relation between shear stress and shear rate depends on its previous history.

(3) viscoelastic fluids which exhibit partial elastic recovery after deformation.

The steady-state rheological behavior of the time-independent fluids may be described by the equation of the form:

$$\tau_{yx} = -\eta \frac{du}{dy} \qquad (1\text{-}1)$$

where η is the non-Newtonian viscosity and may be expressed as a function of either the shear rate (-du/dy) or the shear stress (τ_{yx}). η may be represented by the slope at a given point of the so-called " flow curve ", i.e. the diagram relating shear stress and shear rate for non-Newtonian fluids. Time-independent fluids can further be divided into three distinct groups: (1) Bingham plastics, (2) pseudoplastic fluids and (3) dilatant fluids.

Bingham plastics have a flow curve which, like that of Newtonian fluids, is a straight line but does not pass through the origin. The slope of the straight line gives the plastic viscosity, μ_o. The Bingham model which expresses the rheological relation between the shear stress (τ_{yx}) and the shear rate (-du/dy) may be written as:

$$\tau_{yx} = -\mu_o \frac{du}{dy} \pm \tau_o \qquad \text{if} \quad |\tau_{yx}| > \tau_o \qquad (1\text{-}2)$$

$$\frac{du}{dy} = 0 \qquad \text{if} \quad |\tau_{yx}| < \tau_o \qquad (1\text{-}3)$$

where τ_o is the yield stress. When the shear stress is less than the yield stress the structure of the fluid remains rigid, but when the shear stress exceeds τ_o, the structure disintegrates completely, and the fluid flows like Newtonian. Examples of Bingham plastics are oil paints and pasty materials.

Pseudoplastic fluids have a non-Newtonian viscosity (η) which decreases with increasing rate of shear (-du/dy), but for dilatant fluids η increases with increasing shear rate. The rheological behavior of both types of fluids can be described by the following models:

The Ostwald-de Waele model (or the power-law model)

$$\tau_{yx} = -M \left|\frac{du}{dy}\right|^{n-1} \frac{du}{dy} \qquad (1\text{-}4)$$

The Eyring model

$$\tau_{yx} = A \arcsin\left(-\frac{1}{B}\frac{du}{dy}\right) \qquad (1\text{-}5)$$

The Ellis model

$$-\frac{du}{dy} = \left(\varphi_0 + \varphi_1 \left|\tau_{yx}\right|^{\beta-1}\right)\tau_{yx} \tag{1-6}$$

The Reiner-Philippoff model

$$-\frac{du}{dy} = \left[\frac{1}{\mu_\infty + \dfrac{\mu_0 - \mu_\infty}{1 + (\tau_{yx}/\tau_s)^2}}\right]\tau_{yx} \tag{1-7}$$

With proper choice of the parameter, Eqs. (1-4) to (1-7) can be applied to pseudoplastic, Newtonian, or dilatant fluids. Approximate values of M, n, φ_0, φ_1, β, μ_0, μ_∞, and τ_s for various fluids are tabulated in Bird, Stewart, and Lightfoot (2).

Time-dependent fluids may be subdivided into two classes: (1) thixotropic fluids and (2) rheopectic fluids. The first class includes fluids whose viscosity (η) decreases with time under a suddenly applied constant stress (τ_{yx}), whereas the second are those whose η increases with time. Even though experimental work and theoretical study have been made about time-dependent fluids as well as visco-elastic fluids much of their behavior still remains unknown to engineers.

Since pseudoplastic fluids are most common in industry, this thesis will restrict its investigation to them. It is also found that the power-law model is best adapted because of its simplicity.

CHAPTER II

ASSUMPTIONS AND FUNDAMENTAL EQUATIONS

A. Description of Problem

Fig. 1 gives the schematic description of the problem under investigation. The fluid before entering the duct is assumed to have a uniform velocity profile $u = U_\infty$ and at a uniform temperature T_∞. The walls of the duct are maintained at a constant temperature T_W where $T_W \neq T_\infty$, and the distance between the walls being 2b. Since the lower and upper halves of the conduit are symmetrical to each other, it is only necessary to study either half. For convenience, the origin of the rectangular coordinates is taken at the entrance point of the lower wall with x-axis parallel to the direction of flow and y-axis perpendicular to it. The x-component of the velocity vector is termed u and the y-component v.

B. Assumptions

The assumptions used in this thesis are:

1. The flow is two dimensional.
2. The flow is steady.
3. The fluid is incompressible and has constant physical properties.
4. The dissipative heat due to friction is negligible.

5. The velocity and temperature profiles are flat at the inlet of the duct.
6. There is a thin layer of fluid adjacent to the wall in which the velocity is zero at the wall, but approaches to very near main flow velocity at a distance δ from the wall. This fluid layer is called the velocity boundary layer of thickness δ, and outside this layer, potential flow occurs in the core and the core velocity profile is flat. The velocity boundary layer is assumed to be of zero thickness at the inlet point. It increases in thickness with distance from the inlet point until it reaches the centre line of the duct where the two boundary layers from both walls merge. It is assumed that the viscous effect is confined within the boundary layer, and outside the region the forces due to friction are small and may be neglected.
7. There is a transfer of heat between the fluid and the wall because of the temperature difference. The major part of this transfer takes place in a thin layer of fluid adjacent to the wall. Within the layer temperature varies from T_W at the wall to T_∞ of the undisturbed flow. In an exactly analogous manner to the velocity boundary layer, this thin layer is called the thermal boundary layer of thickness Δ. Outside the thermal boundary layer

the fluid is not materially affected by the heat transfer and the temperature remains the same as that of the fluid before entering. This layer will grow from zero thickness at the inlet point to a value equal to b at the centre line where the two identical thermal boundary layers from both walls meet. It is further assumed that the effect of longitudinal conduction of heat in the fluid is insignificant.

8. The usual boundary layer simplification can be applied to the equations of motion and energy.

C. Basic Equations

For the steady-state laminar flow along the flat duct, the equations of motion, continuity, and energy can be written as follows:

$$u\frac{\partial u}{\partial x} + v\frac{\partial u}{\partial y} = -\frac{1}{\rho}\frac{\partial p}{\partial x} - \frac{1}{\rho}\frac{\partial}{\partial y}(\tau_{yx}) \tag{2-1}$$

$$\frac{\partial p}{\partial y} = 0 \tag{2-2}$$

$$\frac{\partial u}{\partial x} + \frac{\partial v}{\partial y} = 0 \tag{2-3}$$

$$u\frac{\partial T}{\partial x} + v\frac{\partial T}{\partial y} = \alpha\frac{\partial^2 T}{\partial y^2} \tag{2-4}$$

For a non-Newtonian fluid obeying Ostwald-de Waele model, its rheological behavior can be described by

$$\tau = -\left[M \left| \sqrt{\tfrac{1}{2}(\Delta : \Delta)} \right|^{n-1} \right] \Delta \tag{2-5}$$

where M = consistency index

n = flow behavior index

Δ = rate of deformation tensor

values of M and n for various fluids may be found in Bird, Stewart, and Lightfoot (2), Metzner (12) and St. Pierre (13). It should be noted that the flow behavior index (n) is a measure of the degree of non-Newtonian behavior. The farther the value of n deviates from unity, the more pronounced is the non-Newtonian behavior, and for n = 1, Eq. (1-4) and (2-5) reduces to the Newtonian law of viscosity with $M = \mu$.

For Eq. (2-5) the stress component is given by

$$\tau_{ij} = -\left[M \left| \tfrac{1}{2} I_2 \right|^{\frac{n-1}{2}} \right] \left(\frac{\partial u_i}{\partial x_j} + \frac{\partial u_j}{\partial x_i} \right) \tag{2-6}$$

where I_2, the second invariant of stress tensor, is given as:

$$I_2 = \sum_i \sum_j \left[\frac{\partial u_i}{\partial x_j} + \frac{\partial u_j}{\partial x_i} \right]^2 \tag{2-7}$$

In the core, the flow is assumed to be nonviscous and the equation of motion, Eq. (2-1), reduces to

$$U \frac{dU}{dx} = -\frac{1}{\rho} \frac{dp}{dx} \tag{2-8}$$

Combining Eqs. (2-6), (2-7), (2-8) and (2-1), the equation of motion can be simplified to

$$u\frac{\partial u}{\partial x} + v\frac{\partial u}{\partial y} = U\frac{dU}{dx} + \frac{M}{\rho}\frac{\partial}{\partial y}\left\{\left[\left(\frac{\partial u}{\partial y}\right)^2\right]^{\frac{n-1}{2}}\frac{\partial u}{\partial y}\right\}$$

$$= U\frac{dU}{dx} + \frac{M}{\rho}\frac{\partial}{\partial y}\left[\left(\frac{\partial u}{\partial y}\right)^n\right] \qquad (2\text{-}9)$$

CHAPTER III

DEVELOPMENT OF VELOCITY PROFILE

A. Solution of the Equation of Motion

The momentum integral method of von Karman and Pohlhausen (14) is used for the approximate solution of Eq. (2-9). It has been assumed that there exists a finite boundary layer of thickness $\delta(x)$ such that the viscous effect is within that layer; and for $y \geq \delta$, the velocity is uniform and is known as the core velocity. Integrating Eq. (2-9) from $y = 0$ to $y = \delta$, we have

$$\int_0^\delta u\frac{\partial u}{\partial x}dy + v\int_0^\delta \frac{\partial u}{\partial y}dy = \int_0^\delta U\frac{dU}{dx}dy + \int_0^\delta \frac{M}{\rho}\frac{\partial}{\partial y}\left[\left(\frac{\partial u}{\partial y}\right)^n\right]dy \qquad (3\text{-}1a)$$

From the equation of continuity [Eq. (2-3)],

$$v = -\int_0^y \frac{\partial u}{\partial x}dy$$

Substitute v into Eq. (3-1a) and after rearrangement, we have

$$\frac{d}{dx}\int_0^\delta \left[u(U-u)\right]dy + \frac{dU}{dx}\int_0^\delta (U-u)\,dy$$

$$= -\frac{M}{\rho}\int_0^\delta \frac{\partial}{\partial y}\left(\frac{\partial u}{\partial y}\right)^n dy$$

$$= -\frac{M}{\rho}\left[\left(\frac{\partial u}{\partial y}\right)^n_{y=\delta} - \left(\frac{\partial u}{\partial y}\right)^n_{y=0}\right]$$

But $\frac{\partial u}{\partial y} = 0$ at $y = \delta$.

therefore the momentum integral equation is obtained in the form

$$\frac{d}{dx}\int_0^\delta \left[u(U-u)\right]dy + \frac{dU}{dx}\int_0^\delta (U-u)\,dy = \frac{M}{\rho}\left[\left(\frac{\partial u}{\partial y}\right)^n_{y=0}\right] \tag{3-1}$$

A polynomial of the fourth degree is assumed for the velocity distribution, u(y), inside the boundary layer. This is given by

$$\frac{u}{U} = C_1\left(\frac{y}{\delta}\right) + C_2\left(\frac{y}{\delta}\right)^2 + C_3\left(\frac{y}{\delta}\right)^3 + C_4\left(\frac{y}{\delta}\right)^4 \tag{3-2}$$

The coefficients C_1, C_2, C_3 and C_4 can be determined by compatibility conditions which are given as

$$u = 0 \qquad \text{at} \qquad y = 0 \tag{3-3}$$

$$u = U \qquad \text{at} \qquad y = \delta \tag{3-4}$$

$$\frac{\partial u}{\partial y} = 0 \qquad \text{at} \qquad y = \delta \tag{3-5}$$

Equation (3-3) is automatically satisfied by Eq. (3-2). Two additional conditions are required for the determination of C_i. They are obtained from the following considerations:

1. The velocity boundary layer thickness, $\delta(x)$, increases along the down-stream direction, and when the upper and lower layers meet, i.e. $\delta = b$, the flow is considered to be fully developed. For a power-law non-Newtonian fluid in laminar flow along a flat duct, the exact fully developed velocity profile (12) is known to be

$$\frac{u}{U} = 1 - \left(1 - \frac{y}{b}\right)^{\frac{n+1}{n}} \tag{3-6}$$

It becomes obvious that any properly assumed dxpression for u such as Eq. (3-2) should be reduced to Eq. (3-6) when $\delta = b$. This provides a simple and direct way to solve for C_i in Eq. (3-2). However, this is only possible for $n = 1$, 1/2 and 1/3; for values of n other than these, we have to seek other means to determine the coefficients C_i. Appendix A.1 gives a sample calculation for the determination of the coefficients C_i by matching Eq. (3-2) with Eq. (3-6).

2. The total volumetric flow rate across the section of the developed profile as calculated by the approximate velocity expression [Eq. (3-2)] should be the same as that calculated by the exact one [Eq. (3-6)]. Thus we have

$$\int_0^b \left[C_1\left(\frac{y}{b}\right) + C_2\left(\frac{y}{b}\right)^2 + C_3\left(\frac{y}{b}\right)^3 + C_4\left(\frac{y}{b}\right)^4\right] dy = \int_0^b \left[1 - \left(1 - \frac{y}{b}\right)^{\frac{n+1}{n}}\right] dy \tag{3-7}$$

3. The kinetic energy of the fluid crossing the section of the developed profile as determined by the approximate and exact expressions should be equal, i.e.:

$$\int_0^b \left[C_1\left(\frac{y}{b}\right) + C_2\left(\frac{y}{b}\right)^2 + C_3\left(\frac{y}{b}\right)^3 + C_4\left(\frac{y}{b}\right)^4\right]^2 dy = \int_0^b \left[1 - \left(1 - \frac{y}{b}\right)^{\frac{n+1}{n}}\right]^2 dy \tag{3-8}$$

Hence Equations (3-4), (3-5), (3-7) and (3-8) complete

the necessary conditions for determinating C_i in the assumed velocity distribution Eq. (3-2) .

From Eq. (3-4) $$C_1 + C_2 + C_3 + C_4 = 1 \tag{3-9}$$

From Eq. (3-5) $$C_1 + 2C_2 + 3C_3 + 4C_4 = 0 \tag{3-10}$$

From Eq. (3-7) $$1 - \frac{n}{1+2n} = \frac{C_1}{2} + \frac{C_2}{3} + \frac{C_3}{4} + \frac{C_4}{5} \tag{3-11}$$

From Eq. (3-8) $$1 - \frac{2n}{1+2n} + \frac{n}{2+3n}$$

$$= C_1\left(\frac{C_1}{3} + \frac{C_2}{4} + \frac{C_3}{5} + \frac{C_4}{6}\right) + C_2\left(\frac{C_1}{4} + \frac{C_2}{5} + \frac{C_3}{6} + \frac{C_4}{7}\right)$$

$$+ C_3\left(\frac{C_1}{5} + \frac{C_2}{6} + \frac{C_3}{7} + \frac{C_4}{8}\right) + C_4\left(\frac{C_1}{6} + \frac{C_2}{7} + \frac{C_3}{8} + \frac{C_4}{9}\right) \tag{3-12}$$

Appendix A.2 gives a sample calculation for determination of C_i by Equations (3-9) to (3-12). It should be noted that the above equations fail to determine C_i for $n < 0.11355$, because the fourth power polynomial approximation of the velocity distribution is no longer sufficient to describe the flow behavior.

Numerical values of C_i for various values of the flow behavior index (n) are given in Table 1 and Fig. 2. A comparison between the assumed expression for u at fully developed condition and that of the exact for $n = 3/4$, $1/4$ and $1/5$ is shown in Fig. 3. The fully developed velocity profiles are reproduced in the form $u/\bar{U}$ vs. n in Fig. 4.

The non-Newtowian fluid enters the duct at a uniform velocity (U_∞). As the fluid moves along the duct,

the fluid within the velocity boundary layer near the wall is retarded due to the viscous effect, while the fluid in the core will be accelerated from the initial uniform velocity to a final velocity which is attained when the two boundary layers meet at the center line. This continuity requirement can be expressed as

$$\bar{U} b = \int_0^{\delta} u \, dy + U(b - \delta) \tag{3-13}$$

where $\bar{U}$ = average velocity of fluid

or $$b(U - \bar{U}) = \int_0^{\delta} (U - u) \, dy$$

$$= U\delta\left(1 - \frac{C_1}{2} - \frac{C_2}{3} - \frac{C_3}{4} - \frac{C_4}{5}\right)$$

or $$U\delta = \frac{b}{K_1}(U - \bar{U}) \tag{3-14}$$

where $$K_1 = 1 - \frac{C_1}{2} - \frac{C_2}{3} - \frac{C_3}{4} - \frac{C_4}{5} \tag{3-15}$$

When the approximate velocity expression [Eq. (3-2)] is substituted into the momentum integral equation [Eq. (3-1)], and after integration, we have

$$\frac{d}{dx}(K_2 U^2 \delta) + \frac{dU}{dx}(K_1 U \delta) = \frac{M}{\rho} \frac{U^n C_1^n}{\delta^n} \tag{3-16}$$

where $$K_2 = \frac{C_1}{2} + \frac{C_2}{3} + \frac{C_3}{4} + \frac{C_4}{5} - \frac{C_1^2}{3} - \frac{C_2^2}{5} - \frac{C_3^2}{7}$$

$$- \frac{C_4^2}{9} - \frac{C_1 C_2}{2} - \frac{2 C_1 C_3}{5} - \frac{C_1 C_4}{3} - \frac{C_2 C_3}{3}$$

$$- \frac{2 C_2 C_4}{7} - \frac{C_3 C_4}{4} \tag{3-17}$$

Substitute Eq. (3-14) into Eq. (3-16) and carry out the operation:

$$\left[\frac{K_2 b}{K_1}(2U-\bar{U}) + b(U-\bar{U})\right]\frac{dU}{dx} = \left[\frac{M\ U^{2n} C_1^{\,n} K_1^{\,n}}{\rho\ b^n (U-\bar{U})^n}\right]$$

or $$dx = \frac{\rho\, b^{n+1}(U-\bar{U})^n}{M\, U^{2n} C_1^{\,n} K_1^{\,n}}\left[\left(\frac{2K_2+K_1}{K_1}\right)U - \left(\frac{K_2+K_1}{K_1}\right)\bar{U}\right]dU \tag{3-18}$$

If the following transformations are made,

$$U^* = \frac{U}{\bar{U}} \tag{3-19}$$

$$Re_b = \frac{\rho\, b^n\, \bar{U}^{2-n}}{M} \tag{3-20}$$

$$x^* = \frac{x}{b\ Re_b} \tag{3-21}$$

$$\delta^* = \frac{\delta}{b} \tag{3-22}$$

Eq. (3-18) becomes

$$\frac{dx^*}{dU^*} = \frac{(U^*-1)^n}{C_1^{\,n}\ K_1^{\,n}}\left[\left(\frac{K_1+2K_2}{K_1}\right)U^* - \left(\frac{K_1+K_2}{K_1}\right)\right]\frac{1}{U^{*2n}} \tag{3-23}$$

Eq. (3-14) can also be written as

$$\delta^* = \frac{1}{K_1}\left(1-\frac{1}{U^*}\right) \tag{3-24}$$

Eq. (3-23) was integrated numerically by the method of Clippinger and Dimsdale over the interval $x^* = 0$ and $U^* = 1$ to U^*= fully developed value, i.e. $\delta^* = 1$. Appendix B gives a sample calculation. Table 2 gives the results of

U^* and δ^* as a function of x^* for $n = 1/4$, $1/2$ and $3/4$; and these are also presented graphically in Fig. 5 and 6.

In the neighborhood of the entrance section, $x^* = 0$ and $U^* = 1$; Eq. (3-23) is integrated to be

$$U^* - 1 = \left[\frac{C_1^{\,n} K_1^{\,n+1}(1+n)}{K_2} x^*\right]^{\frac{1}{1+n}} \tag{3-25}$$

At the fully developed section, $\delta^* = 1$; Eq. (3-24) becomes

$$U^* = \frac{1}{1 - K_1} \tag{3-26}$$

Other expressions may be assumed for the velocity distribution.. For example, u may be assumed to have the following form:

$$\frac{u}{U} = 1 - \left(1 - \frac{y}{\delta}\right)^{\frac{1+n}{n}} \tag{3-27}$$

If it is substituted into the momentum integral equation and similar operation is carried out as shown previously, the following equations are derived:

$$\frac{dx^*}{dU^*} = \frac{(2n+1)^n (U-1)^n}{(3n+2)(n+1)^n}\left[(5n+4)U^* - (4n+3)\right]\frac{1}{U^{*2n}} \tag{3-28}$$

$$\delta^* = \frac{2n+1}{n}\left(1 - \frac{1}{U^*}\right) \tag{3-29}$$

In the neighborhood of the entrance region the solution for the velocity is

$$U^* - 1 = \left[\frac{(3n+2)(n+1)^n}{(2n+1)^n} x^*\right]^{\frac{1}{1+n}} \tag{3-30}$$

The fully developed velocity is given by

$$U^* = \frac{2n+1}{n+1} \tag{3-31}$$

By letting $n = 1$, Eq. (3-23) to (3-31) will be valid for Newtonian fluid flow, and the equations reduce to the forms developed by Sparrow (15).

B. Entrance Length

The axial distance from the inlet to the point where the two boundary layers from the walls meet at the center line is known as the entrance length. Its dimensionless quantity $(x^*)_{ent}$ is obtained as $\delta^* = 1$ or U^* reaches the fully developed value as given by Eq. (3-26) or (3-31). Fig. 7 shows the dependence of $(x^*)_{ent}$ on the flow behavior index (n).

C. Pressure Loss

The pressure drop in the entrance region consists of the resistance due to viscous effect and the pressure loss due to momentum change of the accelerating fluid in the core. The pressure drop between the inlet ($x^* = 0$) and any point within the entrance length $[x^* \leq (x^*)_{ent}]$ can be obtained by integrating Eq. (2-8) with the lower limit taken as $x^* = 0$ and $U^* = 1$. This gives

$$\frac{p_\infty - p}{\rho \bar{U}^2/2} = U^{*2} - 1 \tag{3-32}$$

In the fully developed region, the pressure drop over a length Δx is given by

$$\frac{\Delta p}{\rho \bar{U}^2/2} = 2\left(\frac{1+2n}{n}\right)^n \left(\frac{\Delta x}{b\, Re_b}\right) \tag{3-33}$$

The dependence of the pressure drop on x^* is given in Fig. 8.

Conventionally, the total pressure drop between the inlet and any point in the fully developed region $[x^* \geq (x^*)_{ent}]$ is given as

$$\frac{\Delta p}{\rho \bar{U}^2/2} = 2\left(\frac{1+2n}{n}\right)^n x^* + Cor. \tag{3-34}$$

where "Cor." is the excess pressure due to the entrance effect in addition to the pressure loss from $x^* = 0$ to the point at x^* if the velocity profile is assumed to be fully developed. The correction term "Cor." is represented mathematically by

$$Cor. = \left[(U^*)^2_{\delta^*=1} - 1\right] - 2\left(\frac{1+2n}{n}\right)^n (x^*)_{ent} \tag{3-35}$$

Substitution of Eq. (3-31) into (3-35) gives

$$Cor. = \frac{n(3n+2)}{(n+1)^2} - 2\left(\frac{1+2n}{n}\right)^n (x^*)_{ent} \tag{3-36}$$

The pressure correction factor (Cor.) is plotted in Fig. 9 as a function of the flow behavior index (n).

CHAPTER IV

DEVELOPMENT OF TEMPERATURE PROFILE

A. Solution of the Energy Equation

The solution of the temperature distribution is obtained in a similar way. In addition to the existence of a velocity boundary layer, a thermal boundary layer with thickness equal to Δ is assumed to exist in the neighborhood of the wall. The effect of heat transfer between the fluid and the wall is confined within this layer and the temperature of the fluid outside the layer remains unchanged. The energy integral equation is obtained by integrating the energy equation (2-4) from $y = 0$ to $y = \Delta$, and after rearrangement, we have

$$\frac{d}{dx}\int_0^{\Delta} u(T_\infty - T)\,dy = \alpha\left(\frac{\partial T}{\partial y}\right)_{y=0} \tag{4-1}$$

The temperature distribution in the thermal boundary layer is assumed to have the form:

$$T^* = \frac{T - T_W}{T_\infty - T_W} = \frac{3}{2}\left(\frac{y}{\Delta}\right) - \frac{1}{2}\left(\frac{y}{\Delta}\right)^3 \tag{4-2}$$

which satisfies the following boundary conditions:

$$T = T_W \quad \text{at} \quad y = 0 \tag{4-3}$$

$$T = T_\infty \quad \text{at} \quad y = \Delta \tag{4-4}$$

$$\frac{\partial T}{\partial y} = 0 \quad \text{at} \quad y = \Delta \tag{4-5}$$

Eq. (3-2) and (4-2) can be substituted into (4-1) which in turn will lead to an expression for Δ. However, the integral on the left hand side of Eq. (4-1) would yield different expressions depending on the relative magnitude of δ and Δ. These will be treated seperately:

Case (a) $\Delta > \delta$

The velocity profile is given by

$$\frac{u}{U} = C_1\left(\frac{y}{\delta}\right) + C_2\left(\frac{y}{\delta}\right)^2 + C_3\left(\frac{y}{\delta}\right)^3 + C_4\left(\frac{y}{\delta}\right)^4 \qquad \text{for} \quad 0 \leq y \leq \delta \tag{3-2}$$

$$u = U \qquad \text{for} \quad \delta \leq y \leq \Delta \tag{4-6}$$

Hence Eq. (4-1) can be written as

$$\frac{d}{dx}\left[\int_0^{\delta} u(T_\infty - T)\,dy + U\int_0^{\Delta}(T_\infty - T)\,dy\right] = \alpha\left(\frac{\partial T}{\partial y}\right)_{y=0} \tag{4-1b}$$

Substituting Equations (3-2), (4-2) and (4-6) into (4-1b) and carrying out the operation, one has

$$\frac{d}{dx}\left[K_3 U\delta + K_4 U\frac{\delta^2}{\Delta} + K_5 U\frac{\delta^4}{\Delta^3} + \frac{3}{8}U\Delta\right] = \frac{3\alpha}{2\Delta} \tag{4-7}$$

where

$$K_3 = \frac{C_1}{2} + \frac{C_2}{3} + \frac{C_3}{4} + \frac{C_4}{5} - 1 = -K_1 \tag{4-8}$$

$$K_4 = -\frac{C_1}{2} - \frac{3C_2}{8} - \frac{3C_3}{10} - \frac{C_4}{4} + \frac{3}{4} \tag{4-9}$$

$$K_5 = \frac{C_1}{10} + \frac{C_2}{12} + \frac{C_3}{14} + \frac{C_4}{16} - \frac{1}{8} \tag{4-10}$$

Introducing the following dimensionless forms in addition

to those given before [Equations (3-19) to (3-22)],

$$\Delta^* = \frac{\Delta}{b} \tag{4-11}$$

$$Pr = \frac{C_p \rho b \bar{U}}{k\, Re_b} \tag{4-12}$$

Eq. (4-7) becomes

$$\left[K_3 \delta^* + K_4 \frac{\delta^{*2}}{\Delta^*} + K_5 \frac{\delta^{*4}}{\Delta^{*3}} + \frac{3}{8}\Delta^*\right] dU^*$$
$$+ \left[K_3 U^* + 2K_4 \frac{\delta^*}{\Delta^*} U^* + 4K_5 \frac{U^* \delta^{*3}}{\Delta^{*3}}\right] d\delta^*$$
$$+ \left[-K_4 \frac{\delta^{*2}}{\Delta^{*2}} - 3K_5 \frac{\delta^{*4}}{\Delta^{*4}} + \frac{3}{8}\right] U^* d\Delta^*$$
$$= \frac{3\, dx^*}{2\Delta^* Pr} \tag{4-13}$$

From Eq. (3-23), we have

$$dx^* = \frac{(U^*-1)^n \left[\left(\frac{K_1 + 2K_2}{K_1}\right) U^* - \left(\frac{K_1 + K_2}{K_1}\right)\right]}{C_1^n K_1^n U^{*2n}}\, dU^*$$

Also, from Eq. (3-24) we obtain

$$d\delta^* = \frac{dU^*}{K_1 U^{*2}} \tag{4-14}$$

Substituting Eqs.(3-23) and (4-14) into (4-13) and after rearrangement, we obtain

$$\frac{dU^*}{d\Delta^*} = \frac{\left[\frac{3}{8} - K_4\left(\frac{\delta^*}{\Delta^*}\right)^2 - 3K_5\left(\frac{\delta^*}{\Delta^*}\right)^4\right] U^*}{\left\{\frac{3\left[\left(\frac{K_1 + 2K_2}{K_1}\right) U^* - \left(\frac{K_1 + K_2}{K_1}\right)\right]}{2\Delta^* Pr\, C_1^n K_1^n U^{*2n}}\right\}}$$
$$- \left\{K_3 \delta^* + K_4 \frac{\delta^{*2}}{\Delta^*} + K_5 \frac{\delta^{*4}}{\Delta^{*3}} + \frac{3}{8}\Delta^* + \frac{K_3}{K_1 U^*} + \frac{2K_4 \delta^*}{K_1 U^* \Delta^*} + \frac{4K_5 \delta^{*3}}{K_1 U^* \Delta^{*3}}\right\} \tag{4-15}$$

Case (b) $\Delta < \delta$

Since the thermal boundary layer is within the velocity boundary layer, one single expression is required to describe the velocity profile [Eq. (3-2)] in the region $0 \leq y \leq \delta$. Following the same technique as in previous case, we derive the following equation:

$$\frac{dU^*}{d\Delta^*} = \frac{\left[\frac{C_1}{5}\left(\frac{\Delta^*}{\delta^*}\right) + \frac{C_2}{8}\left(\frac{\Delta^*}{\delta^*}\right)^2 + \frac{3C_3}{35}\left(\frac{\Delta^*}{\delta^*}\right)^3 + \frac{C_4}{16}\left(\frac{\Delta^*}{\delta^*}\right)^4\right]U^*}{\left\{\frac{3\left[\left(\frac{K_1+2K_2}{K_1}\right)U^* - \left(\frac{K_1+K_2}{K_1}\right)\right]}{2\Delta^* Pr\, C_1^n K_1^n U^{*2n}}\right\} - \left\{\frac{C_1\Delta^{*2}}{10\,\delta^*} + \frac{C_2\Delta^{*3}}{24\,\delta^{*2}}\right\}}$$

$$\frac{}{-\left\{\frac{3C_3\Delta^{*4}}{140\,\delta^{*3}} + \frac{C_4\Delta^{*5}}{80\,\delta^{*4}} - \frac{C_1\Delta^{*2}}{10K_1U^*\delta^{*2}} - \frac{C_2\Delta^{*3}}{12K_1U^*\delta^{*3}}\right\}}$$

$$\frac{}{-\left\{\frac{9C_3\Delta^{*4}}{140K_1U^*\delta^{*4}} - \frac{C_4\Delta^{*5}}{20K_1U^*\delta^{*5}}\right\}} \qquad (4\text{-}16)$$

B. Numerical Integration of Temperature Solutions

Equation (4-15) or (4-16) will be used in conjunction with the results obtained from Eqs. (3-23) and (3-24) [relationship between U^*, δ^*, and x^*] to obtain a relationship between Δ^* and X^*. Numerical integration of Equations (4-15) and (4-16) are carried out using Runge-Kutta method (9). The initial conditions corresponding to $x^* = 0$ or $U^* = 1$ are $\Delta^* = \delta^* = 0$. However, this leads to the indeterminate form for Δ^*/δ^* or δ^*/Δ^*. In order to overcome this difficulty, computation will not start exactly at the entrance point, but a small distance down-stream. Since in the immediate neighborhood of the entrance point U^* is almost unity. Consequently, the flow may be assumed to be the same as that over a flat plate. The solution of velocity and temperature distributions over a flat plate for power-law non-Newtonian fluid has been studied by Acrivos et al. Their results on heat transfer rate and shear stress, expressed in terms of thermal boundary layer thickness and velocity boundary layer thickness, are

$$\delta^* = \left[\frac{(n+1)\,C_1^{\,n}}{K_2}\right]^{\frac{1}{1+n}} x^{*\,\frac{1}{1+n}} \tag{4-17}$$

$$\Delta^* = \frac{2.658681}{\sqrt{Pr}}\, x^{*\,\frac{1}{2}} \qquad \text{for } x^* < x_1^* \tag{4-18}$$

$$\Delta^* = 1.3395\left[\frac{K_6^{\frac{1}{n}}\, Pr}{18}\left(\frac{1+2n}{1+n}\right)\right]^{-\frac{1}{3}} x^{*\,\frac{2+n}{3(1+n)}}$$

$$\text{for } x^* > x_1^* \tag{4-19}$$

$$x_1^* = \left\{ \frac{2.658681}{1.3395 (Pr)^{\frac{1}{3}}} \left[\frac{K_6^{\frac{1}{n}} (1+2n)}{18 \quad (1+n} \right]^{\frac{1}{3}} \right\}^{6\left(\frac{1+n}{1-n}\right)} \tag{4-20}$$

where $$K_6 = \left[\frac{39}{280} \left(\frac{1.5}{1+n} \right) \right]^{\frac{n}{1+n}} \tag{4-21}$$

Appendix C gives the detailed derivation of these expressions.

In the immediate neighborhood of the entrance region, Eq. (3-25) is valid to determine the starting value of U^*:

$$U^* = \left[\frac{C_1^{\,n} K_1^{\,1+n} (1+n)}{K_2} x^* \right]^{\frac{1}{1+n}} - 1 \tag{3-25}$$

Equations (4-17) to (4-21) and (3-25) provide sufficient relationships to start the numerical integration of $dU^*/d\Delta^*$. Computation starts at $\Delta^* = 1 \times 10^{-4}$. This value of Δ^* will give two values of x^*, one from Eq. (4-18) and the other Eq. (4-19). The correct x^* should be chosen from the appropiate equation satisfying the limiting conditions, $x^* < x_1^*$ or $x^* > x_1^*$. Once the value of x^* is known, other values for δ^* and U^* can be calculated. The relative magnitudes of δ^* and Δ^* ($\Delta^* = 1 \times 10^{-4}$) will determine either Eq. (4-15) or (4-16) should be used to continue the integration. In usual cases Δ^* is greater than δ^* in the inlet region so that Eq.(4-15) is integrated first. But somewhere down-stream the ratio of δ^*/Δ^* becomes greater than unity, and a switch to Eq. (4-16) is necessary. Actual computation was carried out by a LGP-30 digital computer. Computation stops when either Δ^* or δ^* reaches unity.

In cases where δ^* first reaches unity, the subsequent growth of Δ^* can be obtained from Eq. (4-1) using the fully developed velocity profile [namely replacing δ by b in Eq. (3-2)]. The resultant equation is found to be

$$\frac{1}{1-K_1}\left\{\frac{C_1}{15}\left[\Delta^{*3}-(\Delta^*)^3_{\delta^*=1}\right]+\frac{C_2}{32}\left[\Delta^{*4}-(\Delta^*)^4_{\delta^*=1}\right]\right.$$
$$\left.+\frac{3C_3}{175}\left[\Delta^{*5}-(\Delta^*)^5_{\delta^*=1}\right]+\frac{C_4}{96}\left[\Delta^{*6}-(\Delta^*)^6_{\delta^*=1}\right]\right\}$$
$$=\frac{3}{2Pr}\left[x^*-(x^*)_{\delta^*=1}\right] \qquad (4\text{-}22)$$

An illustrative example of the numerical integration is given in Appendix D. Numerical values of U^* as a function of Δ^*, Pr and n are tabulated in tables ; and if these values are plotted in graphs, (not shown in this thesis) they can be matched with Fig. 5 to obtain the corresponding values of Δ^* and x^*. The final results, Δ^* and x^*, are given in Table 3 and presented in Fig. 10.

CHAPTER V

HEAT TRANSFER CHARACTERISTICS

A. Definition of the Nusselt Number

The Nusselt number is defined as

$$Nu = \frac{bh}{k} = \frac{b\,k\,\left.\frac{\partial T}{\partial y}\right|_{y=0}}{k\,(T_b - T_w)} \tag{5-1}$$

where T_b is the bulk temperature.

If the following dimensionless quantities are introduced,

$$T_b^* = \frac{T_b - T_w}{T_\infty - T_w} \tag{5-2}$$

$$T^* = \frac{T - T_w}{T_\infty - T_w} = \frac{3}{2}\left(\frac{y}{\Delta}\right) - \frac{1}{2}\left(\frac{y}{\Delta}\right)^3 \tag{4-2}$$

$$y^* = \frac{y}{b} \tag{5-3}$$

the Nusselt number becomes

$$Nu = \frac{\left.\frac{\partial T^*}{\partial y^*}\right|_{y^*=0}}{T_b^*} \tag{5-4}$$

T_b can be found from energy balance and is given by

$$\bar{U}\,b\rho\,C_p\,(T_\infty - T_b) = \int_0^x k\left(\frac{\partial T}{\partial y}\right)_{y=0} dx \tag{5-5}$$

The left hand side gives the change of enthalpy of fluid between the entering point and any point x along the axial direction. The right hand side represents the total amount of heat transferred from fluid to wall in this distance.

After rearrangement, Eq. (5-5) becomes

$$\frac{T_\infty - T_b}{T_\infty - T_W} = \frac{k}{\bar{U}\rho c_p b^2}\int_0^x \left(\frac{\partial T^*}{\partial y^*}\right)_{y^*=0} dx$$

$$= \frac{1}{Pr}\int_0^{x^*} \left(\frac{\partial T^*}{\partial y^*}\right)_{y^*=0} dx^*$$

$$= 1 - \frac{T_b - T_W}{T_\infty - T_W}$$

$$= 1 - T_b^*$$

(5-6)

or

$$T_b^* = 1 - \frac{1}{Pr}\int_0^{x^*} \left(\frac{\partial T^*}{\partial y^*}\right)_{y^*=0} dx^* \qquad (5\text{-}7)$$

and

$$\left(\frac{\partial T^*}{\partial y^*}\right)_{y^*=0} = \frac{3}{2\Delta^*} \qquad (5\text{-}8)$$

Combining Equations (5-4), (5-7) and (5-8), we have

$$Nu_x = \frac{\frac{3}{2}\frac{1}{\Delta^*}}{1 - \frac{3}{2Pr}\int_0^{x^*}\frac{dx^*}{\Delta^*}} \qquad (5\text{-}9)$$

B. Calculation of the Local Nusselt Number by Eq. (5-9)

The integral $\int_0^{x^*}\frac{dx^*}{\Delta^*}$ in Eq. (5-9) can be evaluated as follow:

$$\int_0^{x^*}\frac{dx^*}{\Delta^*} = \int_0^{x_1^*}\frac{dx^*}{\Delta^*} + \int_0^{10^{-4}}\frac{dx^*}{\Delta^*} + \int_{10^{-4}}^{x^*}\frac{dx^*}{\Delta^*}$$

for $x_1^* \leq 1\text{x}10^{-4}$ (5-10)

$$\int_0^{x^*} \frac{dx^*}{\Delta^*} = \int_0^{10^{-4}} \frac{dx^*}{\Delta^*} + \int_{10^{-4}}^{x^*} \frac{dx^*}{\Delta^*}$$

for $x_1^* \geq 1\text{x}10^{-4}$ (5-11),

where x_1^* is determined by Eq. (4-20).

The last integral in both equations can be obtained graphically. However, for the other integrals, $\Delta^* \to 0$ as $x^* \to 0$, or $1/\Delta^* \to \infty$; and graphical integration becomes unreliable. On the other hand, in the interval, $0 \leq x^* \leq 10^{-4}$, flow can be assumed as that of a flat plate, and the solutions for flat plate given by Eq. (4-18) and (4-19) can be utilized. For $x_1^* \leq 1\text{x}10^{-4}$, the Eq. (5-10) becomes

$$\int_0^{x^*} \frac{dx^*}{\Delta^*} = \int_0^{x_1^*} \frac{\sqrt{Pr}\ dx^*}{2.658681\sqrt{x^*}} + \int_{x_1^*}^{10^{-4}} \frac{\left[\frac{K_6^{\frac{1}{n}} Pr}{18}\left(\frac{1+2n}{1+n}\right)\right]^{\frac{1}{3}} dx^*}{1.3395\ (x^*)^{\frac{2+n}{3(1+n)}}} + \int_{10^{-4}}^{x^*} \frac{dx^*}{\Delta^*}$$

$$\int_0^{x^*} \frac{dx^*}{\Delta^*} = \frac{(Pr\ x^*)^{\frac{1}{2}}}{1.329340} + \frac{3}{1.3395}\left(\frac{K_6^{\frac{1}{n}} Pr}{18}\right)^{\frac{1}{3}}\left(\frac{1+n}{1+2n}\right)^{\frac{2}{3}}\left[10^{-4} - x_1^*\right]^{\frac{1+2n}{3(1+n)}} + \int_{10^{-4}}^{x^*} \frac{dx^*}{\Delta^*} \qquad (5\text{-}10a)$$

For $x_1^* \geq 1\text{x}10^{-4}$, Eq. (5-11) is given by

$$\int_0^{x^*} \frac{dx^*}{\Delta^*} = \frac{\sqrt{Pr}}{132.934} + \int_{10^{-4}}^{x^*} \frac{dx^*}{\Delta^*} \qquad (5\text{-}11a)$$

If a graph of $\frac{1}{\Delta^*}$ vs. x^* for each Pr and n is plotted, the integral $\int_{10^{-4}}^{x^*} \frac{dx^*}{\Delta^*}$ can be integrated from the graph, and hence the local Nusselt number is obtained. Appendix E gives a sample calculation. The values of Nu_x and x^* are given in Table 4 and also presented in Fig. 11.

CHAPTER VI

DISCUSSION OF RESULTS

A. Velocity Profile

In this thesis the velocity distribution given by Eq. (3-2) coincides with the fully developed profile when $\delta = b$, but its approach is not asymptotic. It is believed that the boundary layer approach is not suitable as velocity becomes fully developed. Collins and Schowalter (5) used another method to obtain more exact expressions. No apparent difference between their results and those obtained in this work is detected when compared.

B. Entrance Length

It has been pointed out that a fully developed velocity profile is defined in this thesis as the profile when $\delta = b$. This means that the velocity approaches its fully developed value finitely. But the actual approach should be asymptotic. Some authors define entrance length differently. They choose the distance required for the centerline velocity to reach an arbitrary percentage (usually 99%) of its fully developed value as the entrance length. This gives an entrance length larger than that obtained by the "finite" definition. In Bogue's work (3) on non-

Newtonian fluid flowing in the entrance of a pipe, it was found that the values of entrance length obtained by the "finite" definition are about half of those by the "asymptotic" definition. Similar remark may be said about flow in a duct, but the ratio between the values of the entrance length may not be half. In Collins and Schowalter's work they used the "asymptotic" definition for entrance length and their values are definitely higher than those obtained here.

It is known in Newtonian fluid flow that 95% of the additional pressure loss is accomplished in one half of the entrance length. Since a pseudoplastic fluid has a flatter profile, its fully developed form is established more quickly than that for a Newtonian fluid. As a result the distance for the velocity development should be shorter. Therefore the "finite" definition of entrance length should be more appropiate when applied to a pseudoplastic fluid.

C. Pressure Drop

Values of the entry pressure drop correction factor "Cor." for different n are lower than those obtained by Collins and Schowalter. This is contrary to expectation. For a given n, their value of entrance length is higher and should give a smaller "Cor." according to (3-36). For Newtonian fluid, "Cor." was found to be 0.584 compared with their value 0.67 and 0.60 reported by Schlichting (14).

D. Temperature Profiles

The smoothness of the Δ^* vs. x^* curves in Fig. 10 indicates that there is no sudden change of slope when Eqs. (4-15) and (4-16) are joined together. This shows that even though each set of these equations is applicable within certain ranges, it will not break down completely if they were used beyond their applicable ranges. Since the velocity and thermal boundary layers are analogous to each other, their growth should follow a general shape, which is quite evident when Fig. 6 and 10 are compared.

No other results are available to test the accuracy of Eqs. (4-15), (4-16) and (4-22). It has been discussed that the boundary layer analysis is not suitable to the development of velocity profile for the region when $\delta^* \to 1$. Can the same be said about boundary layer calculation for Δ when Δ approaches b? No conclusive answer has been found. It is a general belief that the boundary concept will give good results if the interaction of heat transfer between the two walls is negligible.

E. Heat Transfer Characteristics

From Fig. 11, it may be concluded for a fixed value of x^*, the Nusselt number increases with increasing Prandtl number, but decreases with increasing "n". The Nusselt number reaches the same value (about 0.199) when $\Delta^* = 1$,

regardless of the values of Prandtl number and "n". This means that the Nusselt number is independent of the Prandtl number and the flow behavior index (n) once the temperature profile is fully developed. Another observation is that the values of x^* decreases with decreasing Prandtl number for fully developed heat transfer.

CHAPTER VI

CONCLUSION

Laminar flow behavior and heat transfer of pseudo-plastic fluids obeying the power law in the entrance region of a flat duct have been studied. Boundary layer theory is applied in the simultaneous development of velocity and temperature profiles, and solutions are obtained with simplicity by the approximate method of von Karman and Pohlhausen. Numerical values for U^*, δ^*, Δ^* and Nusselt number as a function of x^* are tabulated and plotted for $n = 3/4$, $1/2$ and $1/4$ over the range of Prandtl number from 1 to 200. Other results include entrance length and pressure loss. Comparison between results of this thesis and those of other theoretical analyses reported in the literature is favorable. The simplicity of the approximate method employed here is obvious and certainly an advantage over the time consuming and laborous exact method. No effort is made to compared the theoretical results with those obtained by experimental work since no such findings have ever been published.

BIBLIOGRAPHY

1. Acrivos, A., M.J. Shah, and E.E. Petersen, A.I.Ch.E. Journal, 6, 312 (1960).

2. Bird, R.B., W.E. Stewart, and E.N. Lightfoot, "Transport Phenomena," pp. 10-15 and 101-108, Wiley, New York (1960).

3. Bogue, D.C., Ind. Eng. Chem., 51, 874 (1959).

4. Collatz, L., "The Numerical Treatment of Differential Equations", pp.61-78, Springer-Verlag, Berlin (1960).

5. Collins, M., and W.R. Schowalter, "Behavior of non-Newtonian Fluids in the Inlet Region of a Channel," technical paper published by Princeton University, Princeton, New Jersey.

7. Goldberg, P., M.S. Thesis, Mech. Eng. Dept., M.I.T., Jan., 1958.

8. Kays, W.M., Trans. A.S.M.E., 77, 1265 (1955).

9. Kunz, K.S., "Numerical Analysis," pp. 206-208, McGraw-Hill, New York (1957).

10. Langhaar, H.L. Jour. Appl. Mechanics, 9. No. 2, A-55 (1942).

11. Lyche, B.C., and R.B. Bird, Chem. Eng. Sci., 6, (1957).

12. Metzner, A.B., "Advances in Chemical Engineering, " ed. by T.B. Drew and J.W. Hookes, Jr., Vol. I, pp. 79-150, Academic Press, New York (1956).

13. St. Pierre, C., M.A.Sc. Thesis, Chem. Eng. Dept., Essex College, Assumption University of Windsor, Windsor, Ontario.

14. Schlicting, H., "Boundary Layer Theory," McGraw-Hill, New York (1960).

15. Sparrow, E.M., Nat. Advisory Comm. Aero. Tech. Note 3331 (Jan 1955).

16. Tien, C., Can. Jour. Chem. Eng., 40, No. 3, 130 (June 1962)

17. Tien, C., "Approximate Calculation on Two-Dimensional Boundary Layer of non-Newtonian Fluid," to be published.

18. Tomita, Y., Bulletin of J.S.M.E., 4, 77 (1961).

19. Wilkinson, W.L., "Non-Newtonian Fluids," Pergamon Press, New York (1960).

NOMENCLATURE

Equation numbers given after description refer to equations in which the symbols are first used or thoroughly defined. Dimensions are given in terms of mass (M), length (L), time (t), and temperature (T).

A = constant in Eyring model, Eq. (1-5).

B = constant in Eyring model, Eq. (1-5).

b = half-spacing between parallel walls in the duct, L.

C_1, C_2, C_3 & C_4
= coefficients of the polynomial expression for velocity distribution, Eq. (3-2).

Cor. = Entry Pressure Drop Correction, Eq. (3-35), M/Lt^2.

c_p = heat capacity at constant pressure, L^2/t^2T.

h = heat transfer coefficient, or increment.

I_2 = second invariant of stress tensor, Eq. (2-7).

K_1 = constant, Eq. (3-15).

K_2 = constant, Eq. (3-17).

K_3 = constant, Eq. (4-8).

K_4 = constant, Eq. (4-9).

K_5 = constant, Eq. (4-10).

K_6 = constant, Eq. (4-21).

k = thermal conductivity, ML/t^3T.

k_v = correction term in Appendix D.

M = consistency index, Eqs. (1-4) & (2-5).

Nu = the Nusselt number, Eq. (5-1).

Nu_x = the local Nusselt number, Eq. (5-9).

n = flow behavior index, Eqs. (1-4) & (2-5).

Pr = $(C_p \rho b \bar{U})/(k Re_b)$, the Prandtl number for flow in duct, or

= $(C_p \rho b U_\infty)/(k Re_b)$, the Prandtl number for flow over flat plate.

p = fluid pressure, M/Lt^2.

p_∞ = fluid pressure at entrance point, M/Lt^2.

Re_b = $(\rho b^n \bar{U}^{2-n})/ (M)$, the Reynolds number for flow in duct, or

= $(\rho b^n U_\infty^{2-n}) /(M)$, the Reynolds number for flow over a flat plate.

T = temperature, T.

T^* = dimensionless group, Eq. (4-2).

T_b = bulk temperature of fluid, T.

T_b^* = dimensionless bulk temperature of fluid, Eq. (5-2).

T_w = temperature at wall, T.

T_∞ = temperature of fluid at entrance point of a duct, or temperature of fluid far from surface of a flat plate, T.

U = velocity of fluid in the core, L/t.

$\bar{U}$ = average velocity of fluid, L/t.

U^* = dimensionless velocity component, Eq. (3-19).

U_∞ = velocity of fluid at entrance point of a duct or free-stream velocity of a flat plate, L/t.

u = x-component of fluid velocity vector, L/t.

v = y-component of fluid velocity vector, L/t.

x = rectangular coordinate in the direction of flow, L.

x^* = dimensionless distance, Eq. (3-21).

y = rectangular coordinate perpendicular to the direction of flow

y^* = y/b, dimensionless distance.

α = $k/\rho C_p$, thermal diffusivity, L^2/t.

β = parameter in Ellis model, Eq. (1-6).

Δ = thermal boundary layer thickness, L.

Δ^* = Δ/b, dimensionleaa thermal boundary layer thickness.

Δ = rate of deformation tensor, Eq. (2-5), t^{-1}.

δ = velocity boundary layer thickness, L.

δ^* = δ/b, dimensionless velocity boundary layer thickness.

η = non-Newtonian viscosity, Eq. (1-1), M/Lt.

μ = Newtonian viscosity, M/Lt.

μ_o = parameter in Bingham model, Eq. (1-2), and Reiner-Philippoff model, Eq. (1-7), M/Lt.

μ_∞ = parameter in Reiner-Philippoff model, Eq. (1-7), M/Lt.

ρ = fluid density, M/L^3.

τ_{ij} = shear stress tensor, Eq. (2-6), M/Lt^2.

τ_o = parameter in Bingham model, Eq. (1-2), M/Lt^2.

τ_s = parameter in Reiner-Philippoff model, Eq. (1-7), M/t^2L.

τ_{yx} = shear stress exerted in the x-direction on a fluid surface which is perpendiculat to the y-direction.

φ_0 = parameter in Ellis model, Eq. (1-6), Lt/M.

φ_1 = parameter in Ellis mode, Eq. (1-6), $L\ t^{2\ -1}/M$.

APPENDIX A

SAMPLE CALCULATION FOR DETERMINATION OF COEFFICIENTS C_i IN EQ. (3-2)

1. By matching Eq. (3-2) with (3-6)

Eq. (3-2) is given as

$$\frac{u}{U} = C_1\left(\frac{y}{\delta}\right) + C_2\left(\frac{y}{\delta}\right)^2 + C_3\left(\frac{y}{\delta}\right)^3 + C_4\left(\frac{y}{\delta}\right)^4 \tag{3-2}$$

If $n = 1/2$. Eq. (3-6) is equal to

$$\frac{u}{U} = 1 - \left(1 - \frac{y}{\delta}\right)^3$$

$$= 3\left(\frac{y}{\delta}\right) - 3\left(\frac{y}{\delta}\right)^2 + \left(\frac{y}{\delta}\right)^3 \tag{A-1}$$

Comparing with Eq. (3-2), we have

$$\begin{aligned} C_1 &= 3 \\ C_2 &= -3 \\ C_3 &= 1 \\ C_4 &= 0 \end{aligned} \tag{A-2}$$

2. By Eq. (3-9) to (3-12)

Eq. (3-9), (3-10) and (3-11) can be rearranged to the form

$$C_1 + C_2 + C_3 = 1 - C_4 \tag{A-3}$$

$$C_1 + 2C_2 + 3C_3 = -4C_4 \tag{A-4}$$

$$\frac{C_1}{2} + \frac{C_2}{3} + \frac{C_3}{4} = 1 - \frac{n}{1 + 2n} - \frac{C_4}{5} \tag{A-5}$$

Applying the method of determinant to the above equations, one can obtain expressions for C_1, C_2 and C_3 in terms of C_4 and n. These are

$$C_1 = 6 - \frac{12n}{1+2n} - \frac{2}{5}C_4 \tag{A-6}$$

$$C_2 = -9 + \frac{24n}{1+2n} + \frac{9}{5}C_4 \tag{A-7}$$

$$C_3 = 4 - \frac{12n}{1+2n} - \frac{12}{5}C_4 \tag{A-8}$$

Substitution of Eq. (A-6), (A-7) and (A-8) into (3-11) gives C_4 in terms of n:

$$C_4 = \frac{7875}{4}\left\{ -\left[\frac{1}{175} + \frac{n}{175(1+2n)}\right] \pm \sqrt{\left[\frac{1}{175} + \frac{n}{175(1+2n)}\right]^2 - \frac{8}{7875}\left[\frac{48n^2}{35(1+2n)^2} - \frac{n}{2+3n} - \frac{4n}{35(1+2n)} + \frac{3}{35}\right]}\right\} \tag{A-9}$$

Therefore, once the value of n is chosen, C_4 is first obtained by (A-9), then C_1, C_2 and C_3 can be found by (A-6), (A-7) and (A-8).

For example, if n = 1/4, we have

$$C_4 = \frac{7875}{4}\left\{\left[\frac{1}{175} + \frac{.25}{175(1.5)}\right] \pm \sqrt{\left[\frac{1}{175} + \frac{.25}{175(1.5)}\right]^2 - \frac{8}{7875}\left[\frac{48(.25)^2}{35(1.5)^2} - \frac{.25}{2.75} - \frac{1}{35(1.5)} + \frac{3}{35}\right]}\right\}$$

$$= -2.27642 \quad \text{or} \quad -23.95968 \text{ (invalid)}$$

$$C_3 = 4 - \frac{12(.25)}{1.5} - \frac{12}{5}(2.27642) = 7.46340$$

$$C_2 = -9 + \frac{24(.25)}{1.5} + \frac{9}{5}(2.27642) = 9.09755$$

$$C_1 = 6 - \frac{12(.25)}{1.5} - \frac{2}{5}(2.27642) = 4.91056$$

APPENDIX B

NUMERICAL INTEGRATION OF EQ. (3-23) BY THE METHOD OF CLIPPINGER & DIMSDALE[+]

Sample calculation is based on $n = 1/2$, and Eq. (3-23) becomes

$$\frac{dx^*}{dU^*} = \frac{(U^*-1)^{\frac{1}{2}}}{U^*(.75)^{\frac{1}{2}}}\left\{\left[\frac{.25+2(.107143)}{.25}\right]U^* - \left(\frac{.25+.107143}{.25}\right)\right\}$$

$$= (U^*-1)^{\frac{1}{2}}\left[2.144449 - \frac{1.649576}{U^*}\right] \tag{B-1}$$

The solution is required over the interval $U^* = 1$ to U = fully developed value which is 4/3 by Eq. (3-24) given that $U^* = 1$ at $x^* = 0$.

The expressions involved in the Clippinger and Dimsdale method are listed below:

$$x^*(U_2^*) = x^*(U_0^*) + 2h\, x^{*\prime}(U_0^*) \tag{B-2}$$

$$x^*(U_1^*) = \frac{1}{2}\left[x^*(U_0^*) + x^*(U_2^*)\right] + \frac{h}{4}\left[x^{*\prime}(U_0^*) - x^{*\prime}(U_2^*)\right] \tag{B-3}$$

Simpson's rule,

$$x^*(U_2^*) = x^*(U_0^*) + \frac{h}{3}\left[x^{*\prime}(U_0^*) + 4x^{*\prime}(U_1^*) + x^{*\prime}(U_2^*)\right] \tag{B-4}$$

[+]Method given in reference (9), pp 206-208.

where $x^*(U_i^*)$ = value of x^* when U^* is equal to U_i^*

$x^{*\prime}(U_i^*)$ = value of dx^*/dU^* when U^* is equal to U_i^*

h = increment of U^*

The first few results of Eq. (B-1) are given in Table B.1 where h is chosen to be 0.01.

Table B.1 Partial Solution of Eq. (B-1)

U^*	$(U^*-1)^{\frac{1}{2}}$	$2.144449 - \frac{1.649576}{U^*}$	dx^*/dU^*	x^*
1.00	0	0.49491	0	0
1.01	0.10000	0.51125	0.51125	-1.8641×10^{-4} 3.2993×10^{-4}
1.02	0.14142	0.52726	0.74656	0 8.3560×10^{-4}
1.03	0.17321	0.54296	0.094046	6.4288×10^{-4} 1.6802×10^{-4}
1.04	0.20000	0.55836	0.111672	1.4913×10^{-4} 2.7095×10^{-4}

The computing procedures are:

1. From Eq. (B-1), find dx^*/dU^* at $U^*= 1.0$ which is 0.
2. Applying Eq. (B-2), the first value of $x^*(1.02)$ is found to be 0.
3. Use Eq. (B-3) to obtain a first approximation to $x^*(1.01)$, namely, -1.8641×10^{-4}.

4. Use Simpson's rule, Eq. (B-4), to get a better value for $x^*(1.02)$ which is 8.3560×10^{-4}.
5. Using $x^*(1.02) = 8.3560 \times 10^{-4}$ instead of the old value, $x^*(1.01)$ is recomputed by Eq. (B-2) to obtain 3.2992×10^{-4}.
6. Successive approximations to $x^*(1.01)$ and $x^*(1.02)$ by the above procedure are terminated when no further change takes place.
7. The next two values $x^*(1.03)$ and $x^*(1.04)$ are obtained in exactly the same way from the knowledge of only $x^*(1.02)$. Thus, each step involves a calculation of two new values and entails exactly the same procedure.

Actual computation was carried out by an LGP-30 digital computer. The results are tabulated in Table 2 and presented graphically in Fig. 5.

APPENDIX C

FLAT PLATE ANALYSIS

The boundary layer theory is applied here as in the analysis for flow in the duct. The core velocity is constant and equals the free stream velocity (U_∞). An expression for velocity distribution within the velocity boundary layer is assumed and the momentum integral method is used to obtain relation for velocity boundary thickness. The velocity distribution is given by

$$\frac{u}{U_\infty} = C_1\left(\frac{y}{\delta}\right) + C_2\left(\frac{y}{\delta}\right)^2 + C_3\left(\frac{y}{\delta}\right)^3 + C_4\left(\frac{y}{\delta}\right)^4 \quad \text{for } 0 \leq y \leq \delta \tag{C-1}$$

$$u = U_\infty \quad \text{for } y \geq \delta \tag{C-2}$$

The momentum integral equation is given by

$$\frac{d}{dx}\int_0^\delta u(U_\infty - u)\,dy = \frac{M}{\rho}\left[\left(\frac{\partial u}{\partial y}\right)^n_{y=0}\right] \tag{C-3}$$

When Eq. (C-1) is substituted into Eq. (C-3), we have

$$\delta^{n+1} = \frac{(1+n)M\,C_1^{\,n}U_\infty^{\,n-2}\,x}{K_2\,\rho} \tag{C-4}$$

Transforming Eq. (C-4) into dimensionless quantities as defined before except where $\bar{U}$ is replaced by U_∞ in the dimensionless forms gives

$$\delta^{*\,1+n} = \frac{(1+n)\,C_1^{\,n}\,x^*}{K_2}$$

$$\delta^* = \left[\frac{(1+n)\,C_1^{\,n}}{K_2}\,x^*\right]^{\frac{1}{1+n}} \tag{4-17}$$

Acrivos et al. (1) have investigated the heat transfer problem for non-Newtonian fluid flow over a flat plate. For $n < 1$ and $x \to \infty$ their result, expressed in terms of present variables, is given as

$$\left(\frac{\partial T^*}{\partial y}\right)_{y=0} = \frac{1}{0.8930}\left[\frac{K_6^{\frac{1}{n}}\,Pr}{18}\left(\frac{1+2n}{1+n}\right)\right]^{\frac{1}{3}} \frac{x^{*\,-\frac{2+n}{3(1+n)}}}{b} \tag{C-5}$$

where $$K_6 = \left[\frac{39}{280}\left(\frac{1.5}{1+n}\right)\right]^{\frac{n}{1+n}} \tag{4-21}$$

If a temperature profile is assumed of the form

$$T^* = \frac{T - T_w}{T_\infty - T_w} = \frac{3}{2}\left(\frac{y}{\Delta}\right) - \frac{1}{2}\left(\frac{y}{\Delta}\right)^3 \tag{C-6}$$

we obtain

$$\left(\frac{\partial T^*}{\partial y}\right)_{y=0} = \frac{3}{2\Delta} \tag{C-7}$$

Therefore, combining Equations (C-5) and (C-7), we have in dimensionless form

$$\Delta^* = 1.3395\left[\frac{K_6^{\frac{1}{n}}\,Pr}{18}\left(\frac{1+2n}{1+n}\right)\right]^{-\frac{1}{3}} x^{*\,\frac{2+n}{3(1+n)}}$$

$$\text{for} \quad x^* > x_1^* \tag{4-19}$$

For $n < 1$ and $x \to 0$, the velocity distribution in the boundary may be disregarded and the resulting expression

for Δ^* is

$$\Delta^* = \frac{3}{2}\sqrt{\frac{\pi}{Pr}}\, x^{*\frac{1}{2}} = \frac{2.658681}{\sqrt{Pr}}\, x^{*\frac{1}{2}}$$

for $x^* < x_1^*$ (4-18)

At some point x_1^* the two equation for Δ^* will be joined. By equating Equations (4-18) and (4-19) we can solve for x_1^*,

$$x_1^* = \left\{\frac{2.658681}{1.3395\,(Pr)^{\frac{1}{6}}}\left[\frac{K_6^{\frac{1}{n}}}{18}\left(\frac{1+2n}{1+n}\right)\right]^{\frac{1}{3}}\right\}^{6\left(\frac{1+n}{1-n}\right)} \qquad (4\text{-}20)$$

APPENDIX D

NUMERICAL INTEGRATION OF EQ. (4-15) AND (4-16) BY RUNGE -KUTTA METHOD+

As it has been noted in Ch. 4, integration will not start at the entrance point, but a small distance downstream. In the immediate neighborhood of the entrance point, the flow is assumed to be the same as that over a flat plate. Therefore computation is made to start at $\Delta^* = 10^{-4}$ which is selected because it will give a corresponding value of x^* so small that within this distance the assumption of flat plate behavior is applicable. However, for $\Delta^* = 10^{-4}$, two values of x^*, one from Eq. (4-18) and the other from (4-19) may be obtained. The starting values for integration depend on the correct choice of x^* among these two values. Sample calculation is based on $n = 1/4$ and $Pr = 100$.

From Eq. (4-21)

$$K_6 = \left[\frac{39}{280}\left(\frac{1.5}{1+n}\right)\right]^{\frac{n}{1+n}}$$

$$= \left[\frac{39}{280}\left(\frac{1.5}{1.25}\right)\right]^{\frac{.25}{1.25}}$$

$$= 0.69938$$

+Method given in reference (4), pp 61-78.

From Eq. (4-18)

$$x^* = \left(\frac{\Delta^* \sqrt{Pr}}{2.658681}\right)^2 = \left(\frac{10^{-4}\sqrt{100}}{2.658681}\right)^2 = 1.4147 \times 10^{-7}$$

From Eq. (4-19)

$$x^* = \left\{\frac{\Delta^*}{1.3395}\left[\frac{K_6^{\frac{1}{n}} Pr}{18}\left(\frac{1+2n}{1+n}\right)\right]^{\frac{1}{3}}\right\}^{\frac{3(1+n)}{2+n}}$$

$$= \left\{\frac{10^{-4}}{1.3395}\left[\frac{(.69938)^4 100}{18}\left(\frac{1.5}{1.25}\right)\right]^{\frac{1}{3}}\right\}^{\frac{3.75}{2.25}} = 1.71705 \times 10^{-7}$$

From Eq. (4-20)

$$x_1^* = \left\{\frac{2.658681}{1.3395 (Pr)^{\frac{1}{6}}}\left[\frac{K_6^{\frac{1}{n}}}{18}\left(\frac{1+2n}{1+n}\right)\right]^{\frac{1}{3}}\right\}^{6\left(\frac{1+n}{1-n}\right)}$$

$$= \left\{\frac{2.658681}{1.3395 (100)^{\frac{1}{6}}}\left[\frac{(.69938)^4}{18}\left(\frac{1.5}{1.25}\right)\right]\right\}^{10}$$

$$= 5.81376 \times 10^{-7}$$

Values of x^* from Eq. (4-18) and (4-19) are both smaller than x_1^*. Since Eq. (4-18) is applicable for $x^* < x_1^*$, its x^* value is the correct choice.

From Eq. (4-17)

$$\delta^* = \left[\frac{(n+1) C_1^{\,n}}{K_2} x^*\right]^{\frac{1}{1+n}}$$

$$= \left[\frac{1.25 (4.91056)^{\frac{1}{4}}}{.0757713}(1.41471 \times 10^{-7})\right]^{\frac{1}{1.25}}$$

$$= 4.29256 \times 10^{-5}$$

In the neighborhood of the entrance point, U^* is given by Eq. (3-25)

$$U^* = \left[\frac{C_1^{\,n} K_1^{\,n+1}(1+n)}{K_2} x^*\right]^{\frac{1}{1+n}} + 1$$

$$U^* = \left[\frac{(4.91056)^{\frac{1}{4}}(.166671)^{1.25}(1.25)}{.0757713}(1.41471\times10^{-7})\right]^{\frac{1}{1.25}} + 1$$

$$= 1.0000071$$

Since $\Delta^* = 10^{-4} > \delta^* = 4.29256\text{x}10^{-5}$, Eq. (4-15) should be integrated first. For $n = 1/4$. Eq. (4-15) reduces to

$$\frac{dU^*}{d\Delta^*} = \frac{U^*\left[.375 + .00374823\left(\frac{\delta^*}{\Delta^*}\right)^4 - .0363800\left(\frac{\delta^*}{\Delta^*}\right)^2\right]}{\left\{\left[\frac{1.5(U^*-1)^{0.25}}{\Delta^* Pr}\left(2.00711U^{*\frac{1}{2}} - \frac{1.52919}{U^{*\frac{1}{2}}}\right)\right]\right.}$$

$$\frac{}{+\left[.1666718^* - .0363800\frac{\delta^{*2}}{\Delta^*} + .00124941\frac{\delta^{*4}}{\Delta^{*3}}\right]}$$

$$\frac{}{\left.+\left[-.375\Delta^* + \frac{1}{U^*} - .436547\frac{\delta^*}{U^*\Delta^*} + .0299850\frac{\delta^{*3}}{U^*\Delta^{*3}}\right]\right\}}$$

(D-1)

If the values of Δ^*, δ^* and U^* are substituted into Eq. (D-1), we have

$$\frac{dU^*}{d\Delta^*} = 8.1464648 \times 10^{-2}$$

Hence all the starting values are obtained and we are ready to proceed to the integration of Eq. (4-15).

Eq. (D-1) can be written as

$$\frac{dU^*}{d\Delta^*} = f(U^*, \delta^*, \Delta^*) \qquad \text{(D-2)}$$

and the computing procedure for its integration by Runge-Kutta method may be summarized in the following table:

Table D.1 Runge-Kutta Scheme for the Differential Equation $dU^*/d\Delta^* = f(U^*, \delta^*, \Delta^*)$

Step	Δ^*	U^*	δ^*	$\frac{k_v}{2} = \frac{h}{2} f(U^*, \delta^*, \Delta^*)$	Correction
1	Δ_0^*	U_0^*	δ_0^*	$k_1/2$	$k = \frac{1}{3}\left(\frac{k_1}{2} + k_2 + k_3 + \frac{k_4}{2}\right)$
2	$\Delta_0^* + \frac{1}{2}h$	$U_0^* + \frac{1}{2}k_1$	$\frac{1}{K_1}\left(1 - \frac{1}{U^*}\right)$	$k_2/2$	
3	$\Delta_0^* + \frac{1}{2}h$	$U_0^* + \frac{1}{2}k_2$	$\frac{1}{K_1}\left(1 - \frac{1}{U^*}\right)$	$k_3/2$	
4	$\Delta_0^* + h$	$U_0^* + k_3$	$\frac{1}{K_1}\left(1 - \frac{1}{U^*}\right)$	$k_4/2$	
5	$\Delta_1^* = \Delta_0^* + h$	$U_1^* = U_0^* + k$	$\delta_1^* = \frac{1}{K_1}\left(1 - \frac{1}{U_1^*}\right)$		

where k_v is the correction and h is the increment.

The values in Step 1 are the starting values which were found previously. The increment h should be small but its value may be increased later to speed up the integration. For this example the first increment h is set to be 5×10^{-4}; 10^{-3}, 5×10^{-3}, 10^{-2}, and 2×10^{-2} as integration proceeds.

The values in Step 1 are:

$$\Delta_0^* = 10^{-4} \qquad \delta_0^* = 4.29256 \times 10^{-5}$$

$$U_0^* = 1.0000071$$

$$\frac{dU^*}{d\Delta^*} = 8.1464648 \times 10^{-2}$$

$$k_1/2 = 8.1464648 \times 10^{-6}$$

The values in Step 2 are:

$$\Delta_0^* + \frac{1}{2}h = 10^{-4} + \frac{1}{2}(2 \times 10^{-4})$$
$$= 2 \times 10^{-4}$$

$$U_0^* + \frac{1}{2}k_1 = 1.0000071 + 8.1464648 \times 10^{-6}$$
$$= 1.0000153$$

from Eq. (3-24)

$$\delta^* = \frac{1}{K_1}\left(1 - \frac{1}{U^*}\right)$$

$$= \frac{1}{.166671}\left(1 - \frac{1}{1.0000153}\right)$$

$$= 9.1773805 \times 10^{-5}$$

from Eq. (D-1)

$$\frac{dU^*}{d\Delta^*} = .12072320$$

$$k_2/2 = 1.2072320 \times 10^{-5}$$

The calculation for the other steps follows the same procedure. The actual results of the calculation are given in Step 5 whereas the steps in between are for better approximation. These results in Step 5 serve as starting value for the next Δ_2^* in the continuation of the solution.

When Δ^* becomes less than δ^*, integration is switched to Eq. (4-16). For n = 1/4, Eq. (4-16) reduces to

$$\frac{dU^*}{d\Delta^*} = \frac{U^*\left[.982112\left(\frac{\Delta^*}{\delta^*}\right) - 1.13719\left(\frac{\Delta^*}{\delta^*}\right)^2 + .639720\frac{\Delta^{*3}}{\delta^{*3}}\right]}{\left\{\left[\frac{1.5}{\Delta^* Pr}(U^*-1)^{\frac{1}{4}}\left(2.00711\,U^{*\frac{1}{2}} - \frac{1.52919}{U^{*\frac{1}{2}}}\right)\right]\right.}$$

$$\frac{\left[+ .142276\left(\frac{\Delta^*}{\delta^*}\right)^4\right]\Big\}}{+\left[-.491056\frac{\Delta^{*2}}{\delta^*} + .379064\frac{\Delta^{*3}}{\delta^{*2}} - .15993\frac{\Delta^{*4}}{\delta^{*3}} + .0284552\frac{\Delta^{*5}}{\delta^{*4}}\right]}$$

$$\frac{}{+\left[\frac{2.94626}{U^*}\left(\frac{\Delta^*}{\delta^*}\right)^2 - \frac{4.54866}{U^*}\left(\frac{\Delta^*}{\delta^*}\right)^3 + \frac{2.878670}{U^*}\left(\frac{\Delta^*}{\delta^*}\right)^4 - \frac{.682908}{U^*}\left(\frac{\Delta^*}{\delta^*}\right)^5\right]\Big\}} \qquad \text{(D-3)}$$

In this example, δ^* first reaches unity and the subsequent growth of Δ^* is obtained by Eq. (4-22).

The actual computation was carried out by an LGP-30 digital computer. A programme is set up so the selection of the correct x^* for the starting values, the choice of Eq. (4-15) or (4-16) to be integrated, and the use of Eq. (4-22) to calculate the continued growth of Δ^* are done automatically. Table 5 shows a sample computer results of the integration of Eq. (4-15) and (4-16) for $n = 1/4$ and $Pr = 100$.

APPENDIX E

SAMPLE CALCULATION FOR THE LOCAL NUSSELT NUMBER, Nu_x

In order to find the Nu_x at certain value of x^*, the integral $\int_0^{x^*} \frac{dx^*}{\Delta^*}$ must be determined first. This integral can be calculated either by Eq. (5-10a) or (5-11a) depending whether $x_1^* \leq 10^{-4}$ or $x_1^* \geq 10^{-4}$. If n = 3/4 and Pr = 100, x_1^* as computed by Eq. (4-20) is

$$x_1 = \left\{ \frac{2.658681}{1.3395\,(Pr)^{\frac{1}{6}}} \left[\frac{K_6^{\frac{1}{n}}}{18} \left(\frac{1+2n}{1+n} \right) \right]^{\frac{1}{3}} \right\}^{6\left(\frac{1+n}{1-n}\right)}$$

$$= \left\{ \frac{2.658681}{1.3395\,(100)^{\frac{1}{6}}} \left[\frac{(.40186)^{\frac{4}{3}}}{18} \frac{2.5}{1.75} \right]^{\frac{1}{3}} \right\}^{42}$$

$$= 5.1187 \times 10^{-25}$$

Since $x_1^* = 5.1187 \times 10^{-25} < 10^{-4}$, Eq. (5-10a) is used to determine the integral. Hence

$$\int_0^{x^*} \frac{dx^*}{\Delta^*} = \frac{\sqrt{Pr}\; x^{*\frac{1}{2}}}{1.32934} + \frac{3}{1.3395} \left[\frac{K_6^{\frac{1}{n}} Pr}{18} \right]^{\frac{1}{3}} \left(\frac{1+n}{1+2n} \right)^{\frac{2}{3}} \left[10^{-4} - x_1^* \right]^{\frac{1+2n}{3(1+n)}}$$

$$+ \int_{10^{-4}}^{x^*} \frac{dx^*}{\Delta^*}$$

$$= \frac{\sqrt{100}\,(5.1187 \times 10^{-25})^{\frac{1}{2}}}{1.32934}$$

$$+ \frac{3}{1.3395} \left[\frac{(.40186)^{\frac{4}{3}}\, 100}{18} \right]^{\frac{1}{3}} \left(\frac{1.75}{2.5} \right)^{\frac{2}{3}} \left[10^{-4} - 5.1187 \times 10^{-25} \right]^{\frac{2.5}{4.25}}$$

$$+ \int_{10^{-4}}^{x^*} \frac{dx^*}{\Delta^*}$$

$$\int_0^{x^*} \frac{dx^*}{\Delta^*} = 5.32565 \times 10^{-12} + 2.59679 \times 10^{-2} + \int_{10^{-4}}^{x^*} \frac{dx^*}{\Delta^*}$$

$$= 2.59679 \times 10^{-2} + \int_{10^{-4}}^{x^*} \frac{dx^*}{\Delta^*} \qquad \text{(E-1)}$$

The last integral in Eq. (E-1) is found by graphically integration. The figure below shows a schematic diagram of $1/\Delta^*$ vs. x^* (the diagram drawn to scale is not presented in this thesis):

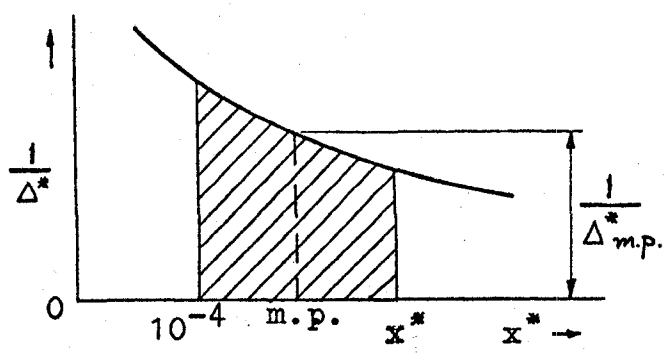

Fig. E.1 Schematic Diagram of $1/\Delta^*$ vs. x^*

where m.p. is the mid-point between 10^{-4} and x^*. Therefore,

$$\int_{10^{-4}}^{x^*} \frac{dx^*}{\Delta^*} \simeq \text{area of shaded section}$$

$$\simeq \frac{1}{\Delta^*_{m.p.}}(x^* - 10^{-4}) \qquad \text{(E-2)}$$

The width of the shaded section should be kept small enough to give good approximation. If $x^* = 2\text{x}10^{-4}$, the mid-point $x^*_{m.p.} = 1.5\text{x}10^{-4}$ and the corresponding value for $1/\Delta^*_{m.p.}$ is found to be 97.0874. By Eq. (E-2),

$$\int_{10^{-4}}^{2\times10^{-4}} \frac{dx^*}{\Delta^*} = 97.0874\,(2\times10^{-4} - 10^{-4})$$

$$= 9.70874 \times 10^{-3}$$

Therefore the integral of Eq. (E-1) is

$$\int_{0}^{2\times10^{-4}} \frac{dx^*}{\Delta^*} = 2.59679\times10^{-2} + 9.70874\times10^{-3}$$

$$= 3.56766\times10^{-2}$$

At $x^* = 2\text{x}10^{-4}$, the value of $\Delta^* = 0.0147$, and the local Nusselt number by Eq. (5-9) will be

$$Nu_{x^*=2\times10^{-4}} = \frac{\frac{3}{2}\,\frac{1}{\Delta^*}}{1 - \frac{3}{2Pr}\int_0^{2\times10^{-4}} \frac{dx^*}{\Delta^*}}$$

$$= \frac{\frac{3}{2}\,\frac{1}{.0147}}{1 - \frac{3\times 3.56766\times10^{-2}}{2\times100}}$$

$$= 125.0663$$

If the next value of Nu_x is wanted at $x^* = 4\text{x}10^{-4}$, the integral of Eq. (E-1) can be written as

$$\int_0^{4\times10^{-4}} \frac{dx^*}{\Delta^*} = \int_0^{2\times10^{-4}} \frac{dx^*}{\Delta^*} + \int_{2\times10^{-4}}^{4\times10^{-4}} \frac{dx^*}{\Delta^*}$$

$$= 3.56766\times10^{-2} + \int_{2\times10^{-4}}^{4\times10^{-4}} \frac{dx^*}{\Delta^*}$$

Following the same procedure as illustrated in the graphical integration for Nu_x at $x^* = 2x10^{-4}$, the integral $\int_{2x10^{-4}}^{4x10^{-4}} \frac{dx^*}{\Delta^*}$ is found to be $1.36054x10^{-2}$.

Hence

$$\int_0^{4\times10^{-4}} \frac{dx^*}{\Delta^*} = 3.56766\times10^{-2} + 1.36054\times10^{-2}$$
$$= 4.92820\times10^{-2}$$

At $x^* = 4x10^{-4}$, $\Delta^* = 0.0170$; and the Nu_x is

$$Nu_{x^*=4\times10^{-4}} = \frac{\frac{3}{2}\left(\frac{1}{.0170}\right)}{1 - \frac{3}{2Pr}\int_0^{4\times10^{-4}} \frac{dx^*}{\Delta^*}}$$
$$= 88.3138$$

Other Nu_x at higher values of x^* is found in the same way; and the calculation is simplified by the additive property of the approximate graphical integration of the integral $\int_0^{x^*} \frac{dx^*}{\Delta^*}$.

APPENDIX F

FIGURES

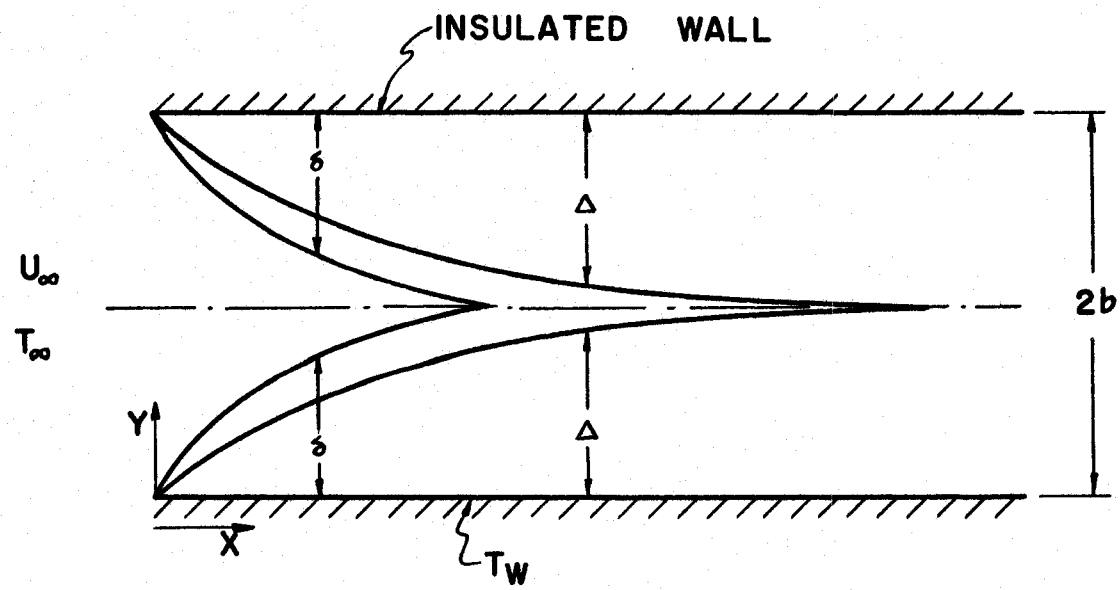

FIG. 1 SCHEMATIC DIAGRAM

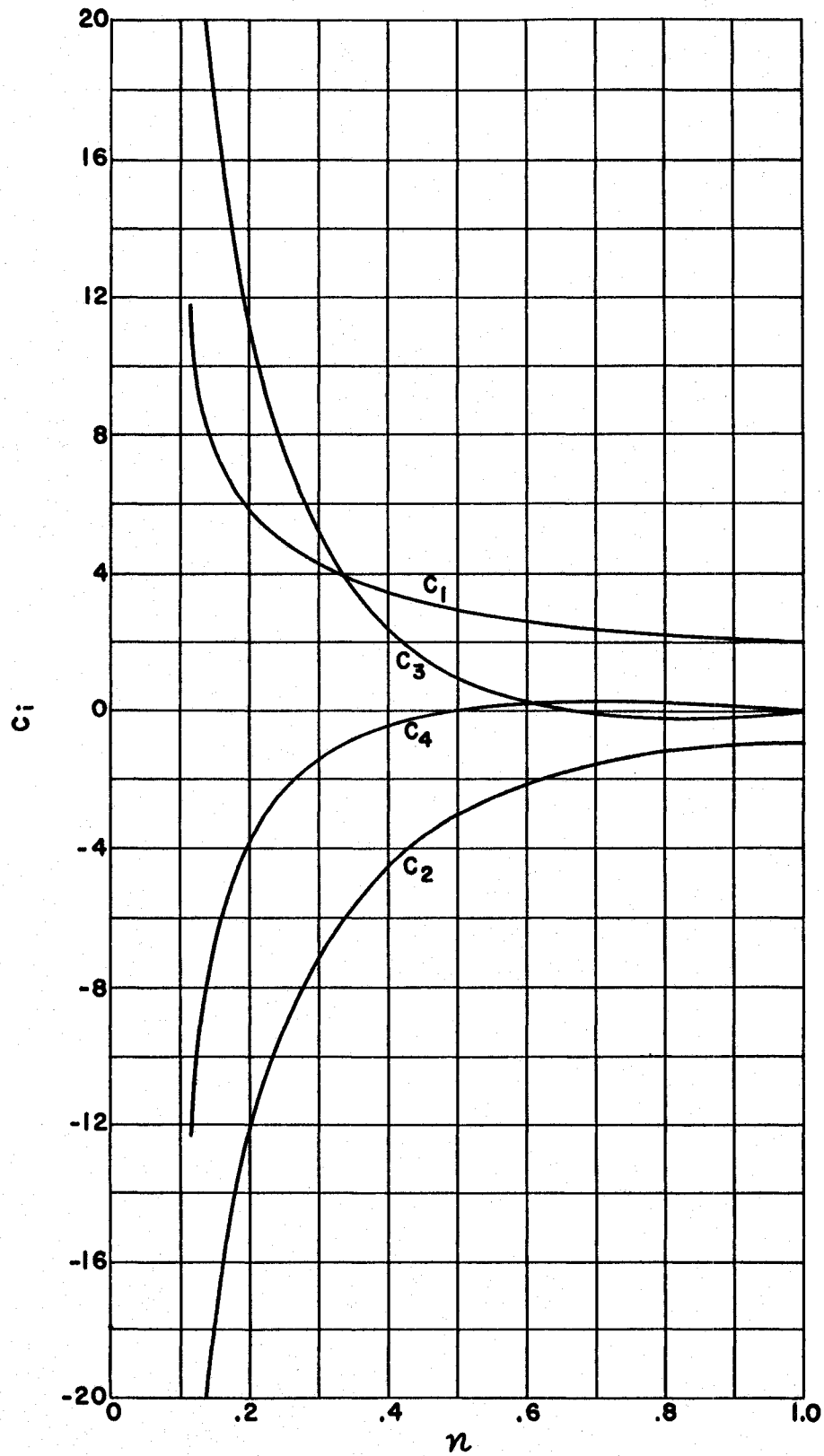

FIG. 2 COEFFICIENTS C_i'S OF THE APPROXIMATE EXPRESSION FOR VELOCITY DISTRIBUTION FOR VARIOUS FLUIDS

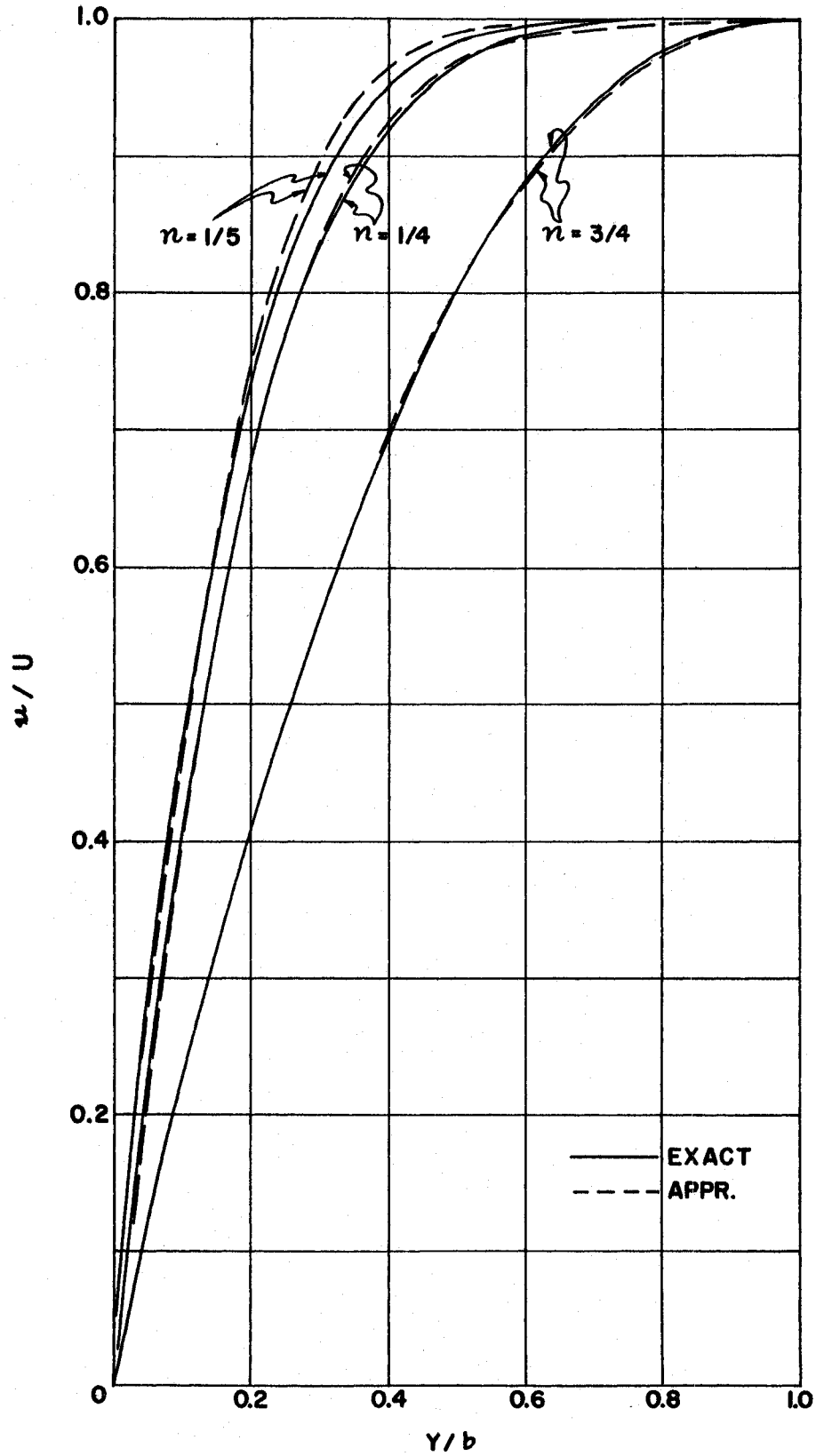

FIG. 3 COMPARISON OF EXACT & APPROXIMATE VELOCITY PROFILES

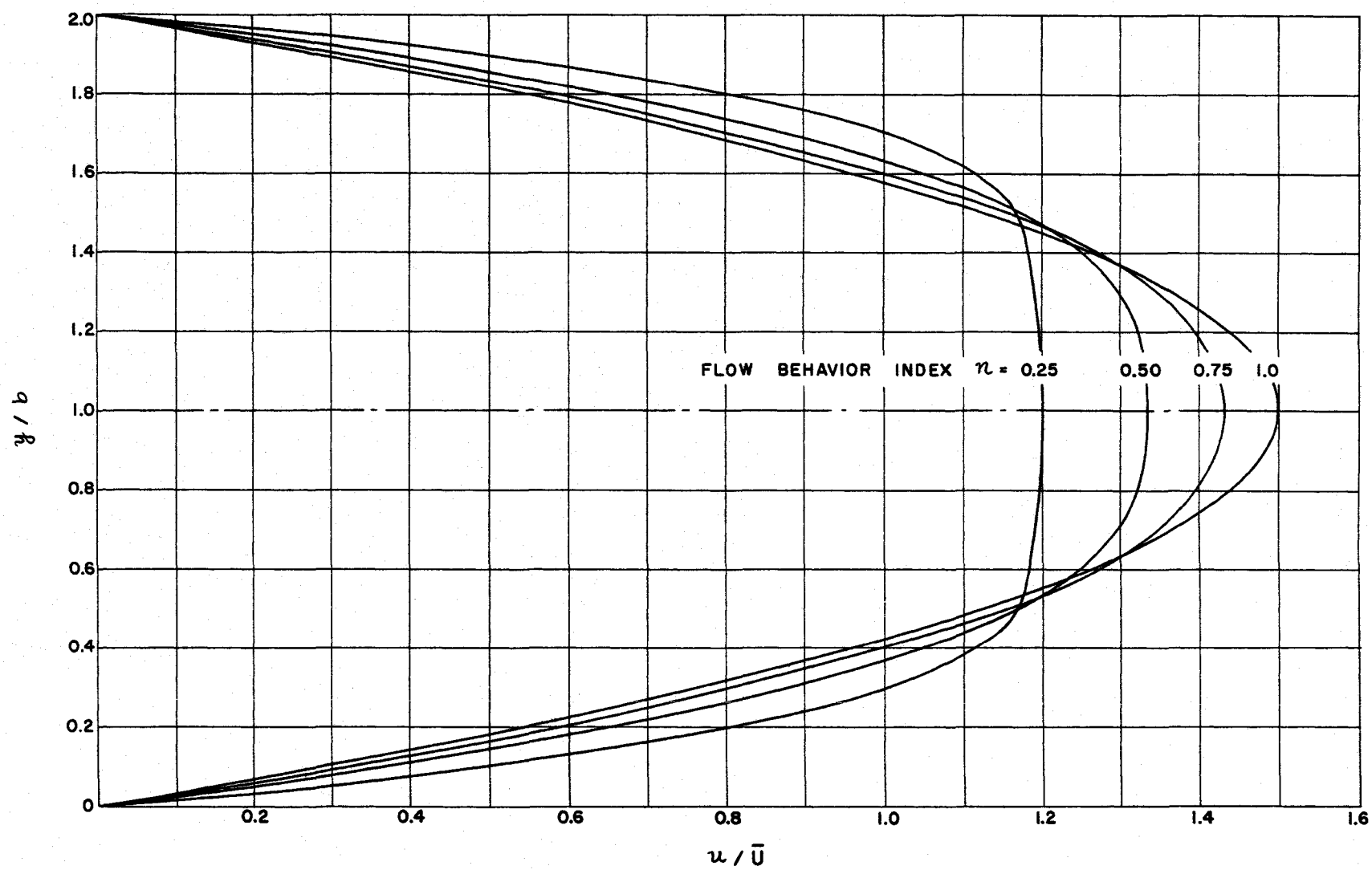

FIG. 4 FULLY DEVELOPED VELOCITY PROFILES

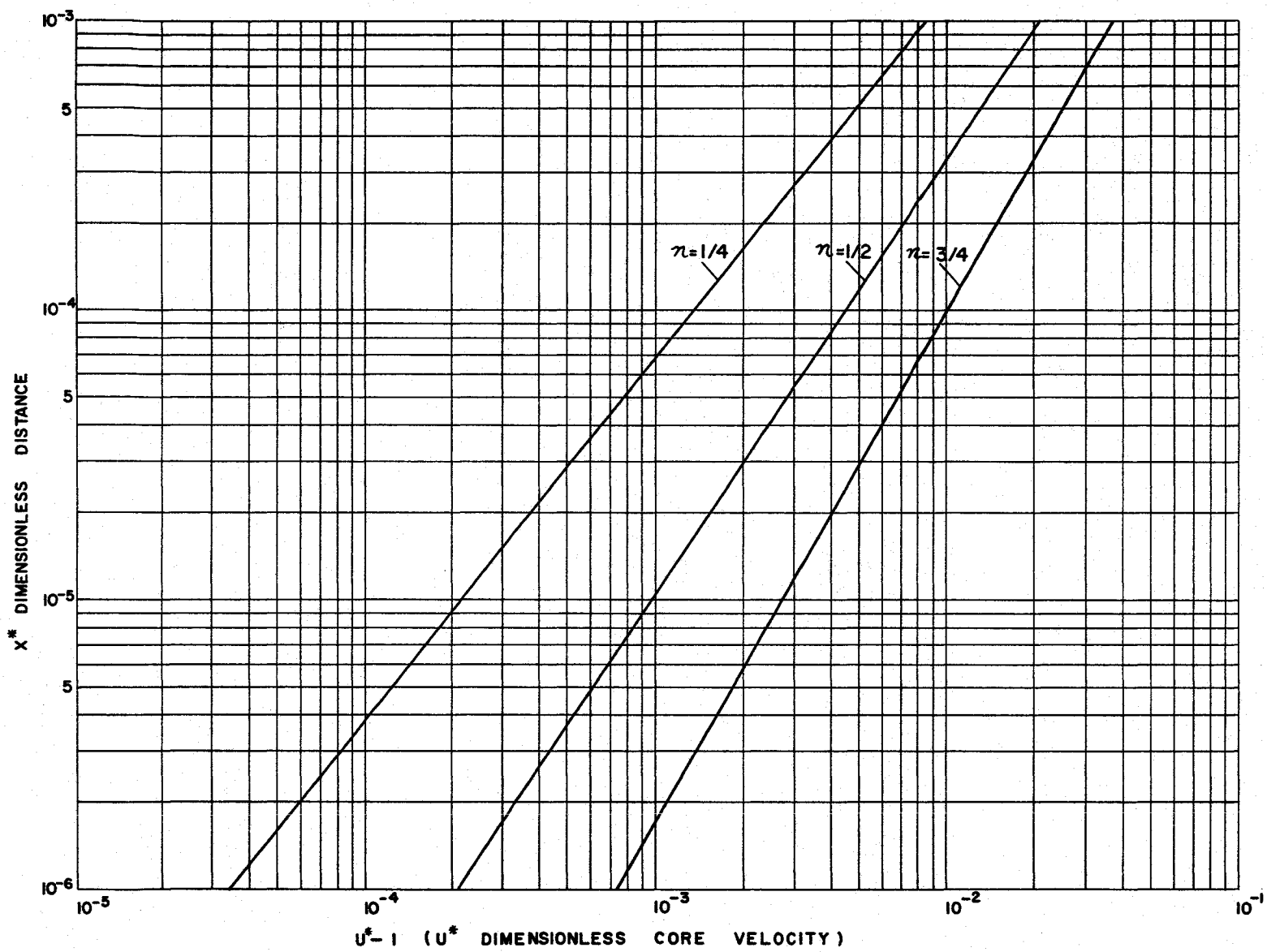

FIG. 5-A, $U^* - 1$ (U^* DIMENSIONLESS CORE VELOCITY) VS. DIMENSIONLESS DISTANCE X^*

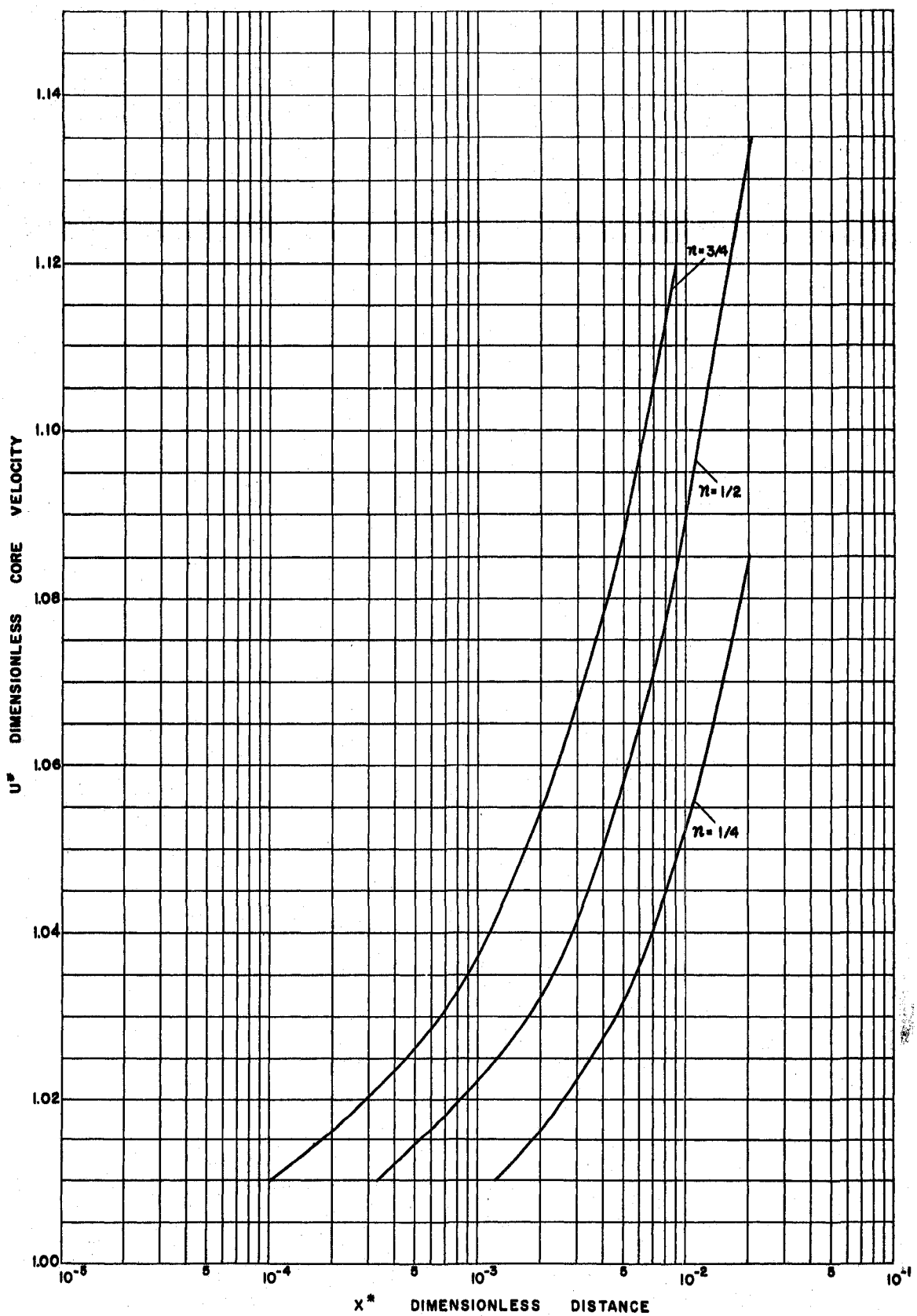

FIG. 5-B DIMENSIONLESS CORE VELOCITY U^* VS. DIMENSIONLESS DISTANCE X^*

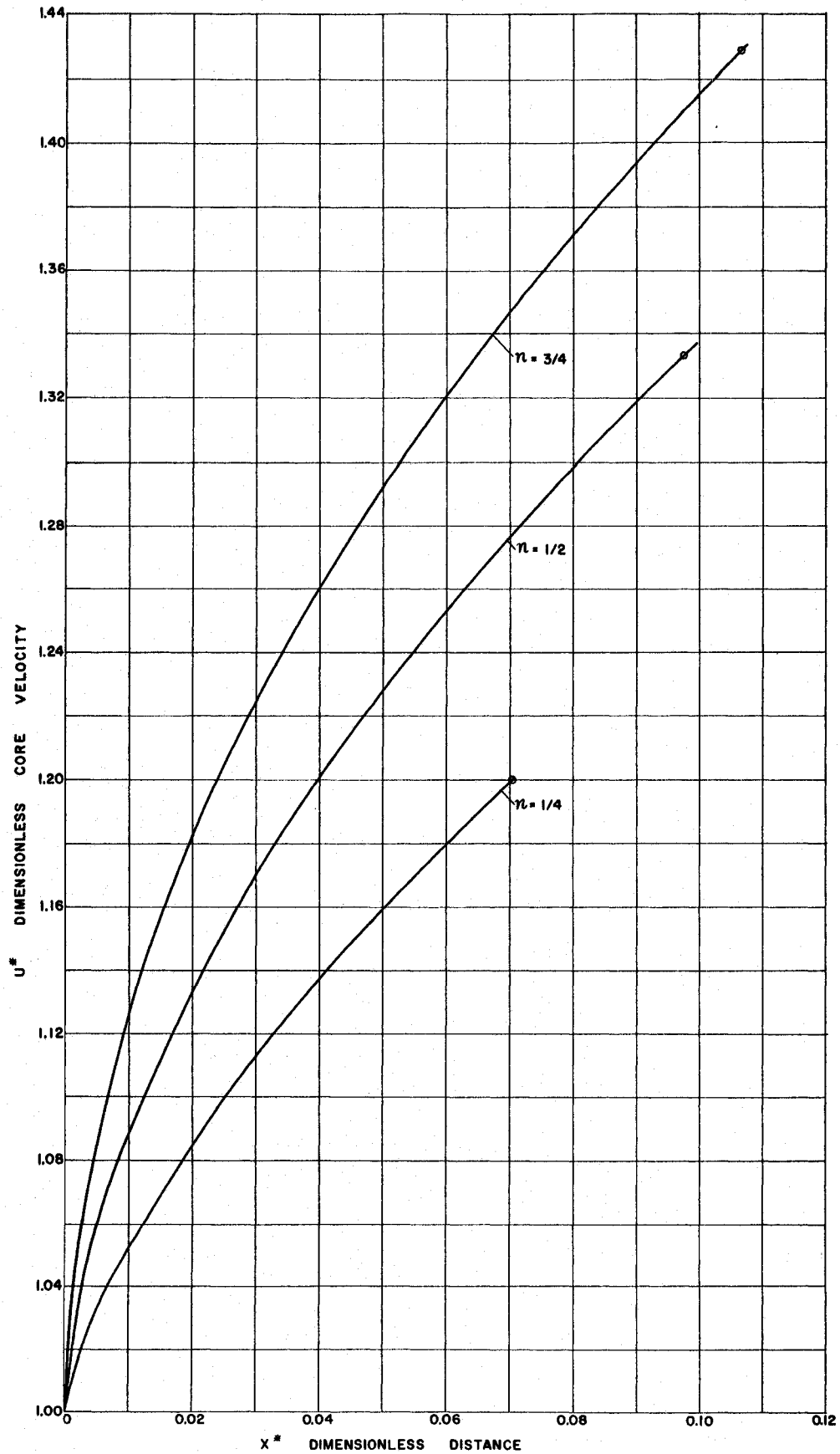

FIG. 5-C DIMENSIONLESS CORE VELOCITY U^* VS. DIMENSIONLESS DISTANCE X^*

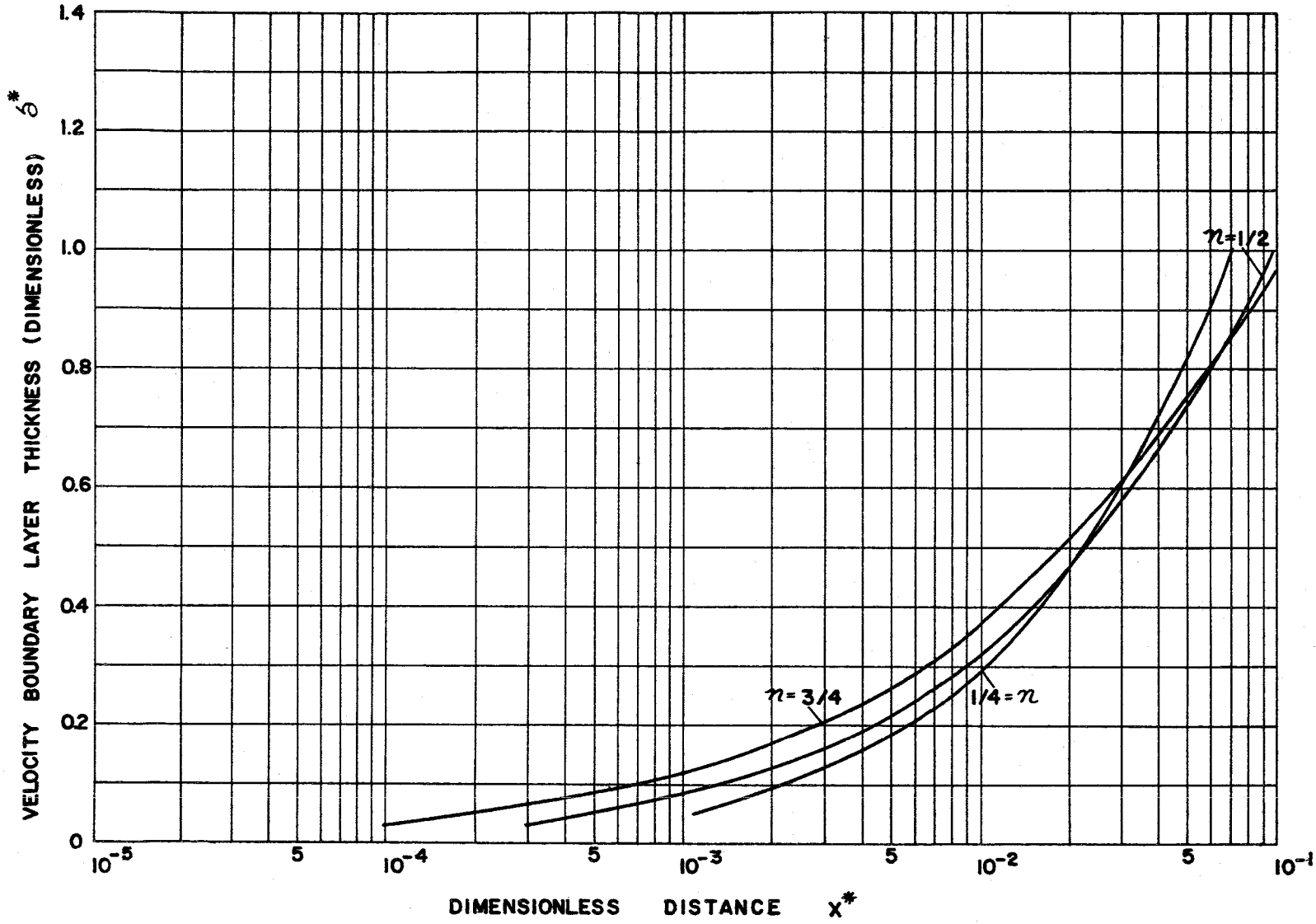

FIG. 6 δ^* DIMENSIONLESS VELOCITY BOUNDARY THICKNESS VS. X^* DIMENSIONLESS DISTANCE

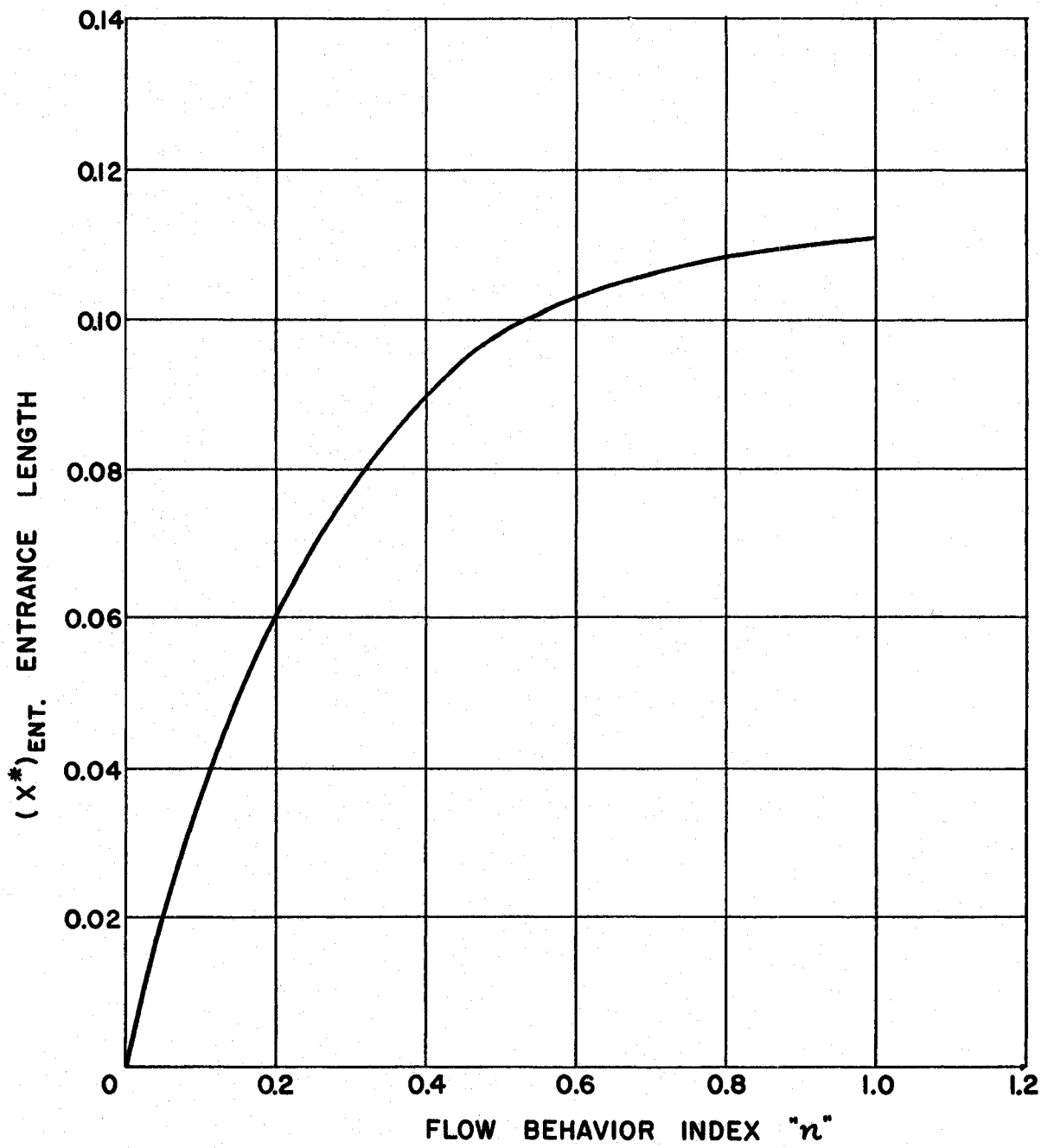

FIG. 7 ENTRANCE LENGTH $(X^*)_{ENT.}$ VS. FLOW BEHAVIOR INDEX "n"

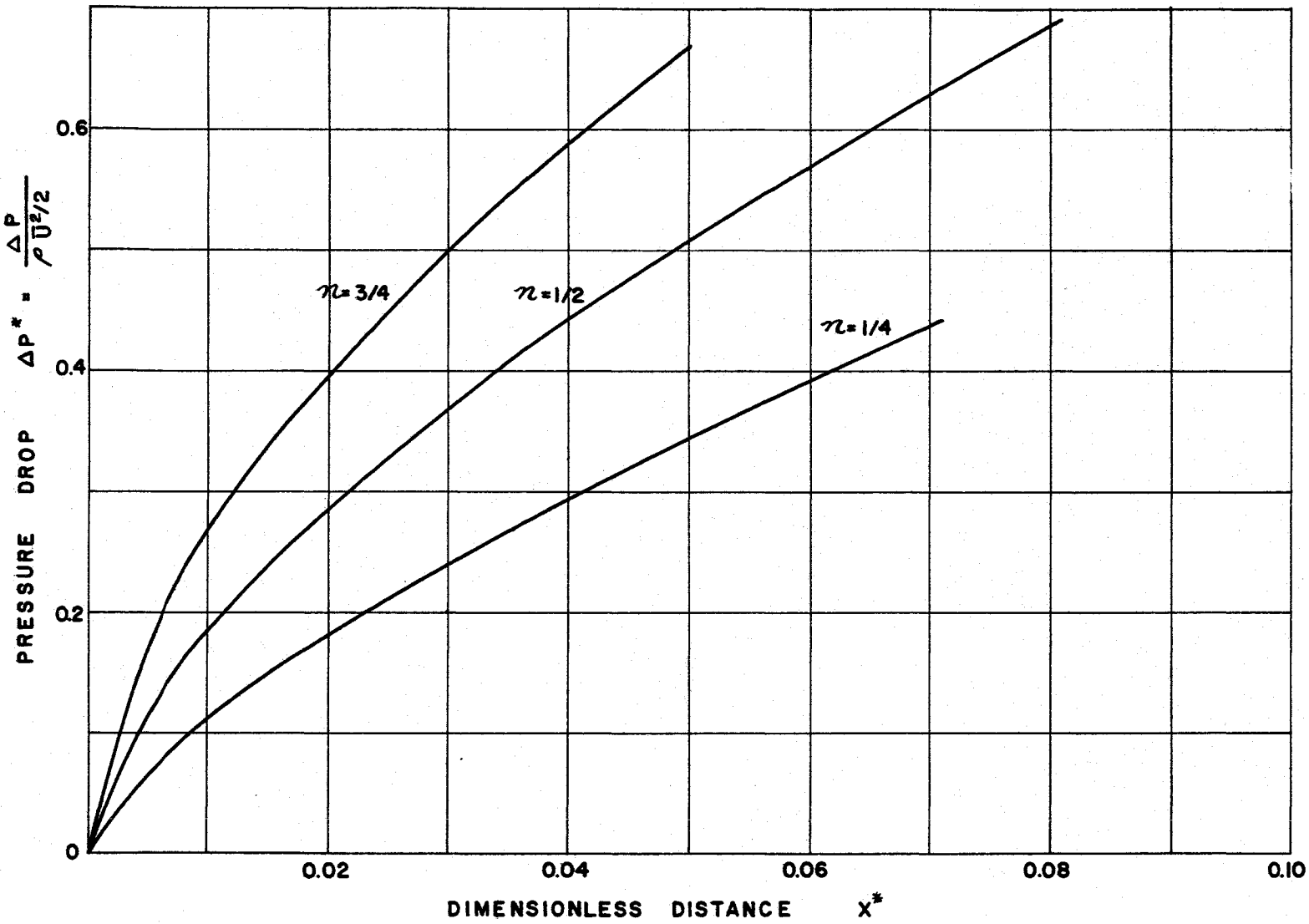

FIG. 8 ΔP^* PRESSURE DROP VS. X^* DIMENSIONLESS DISTANCE

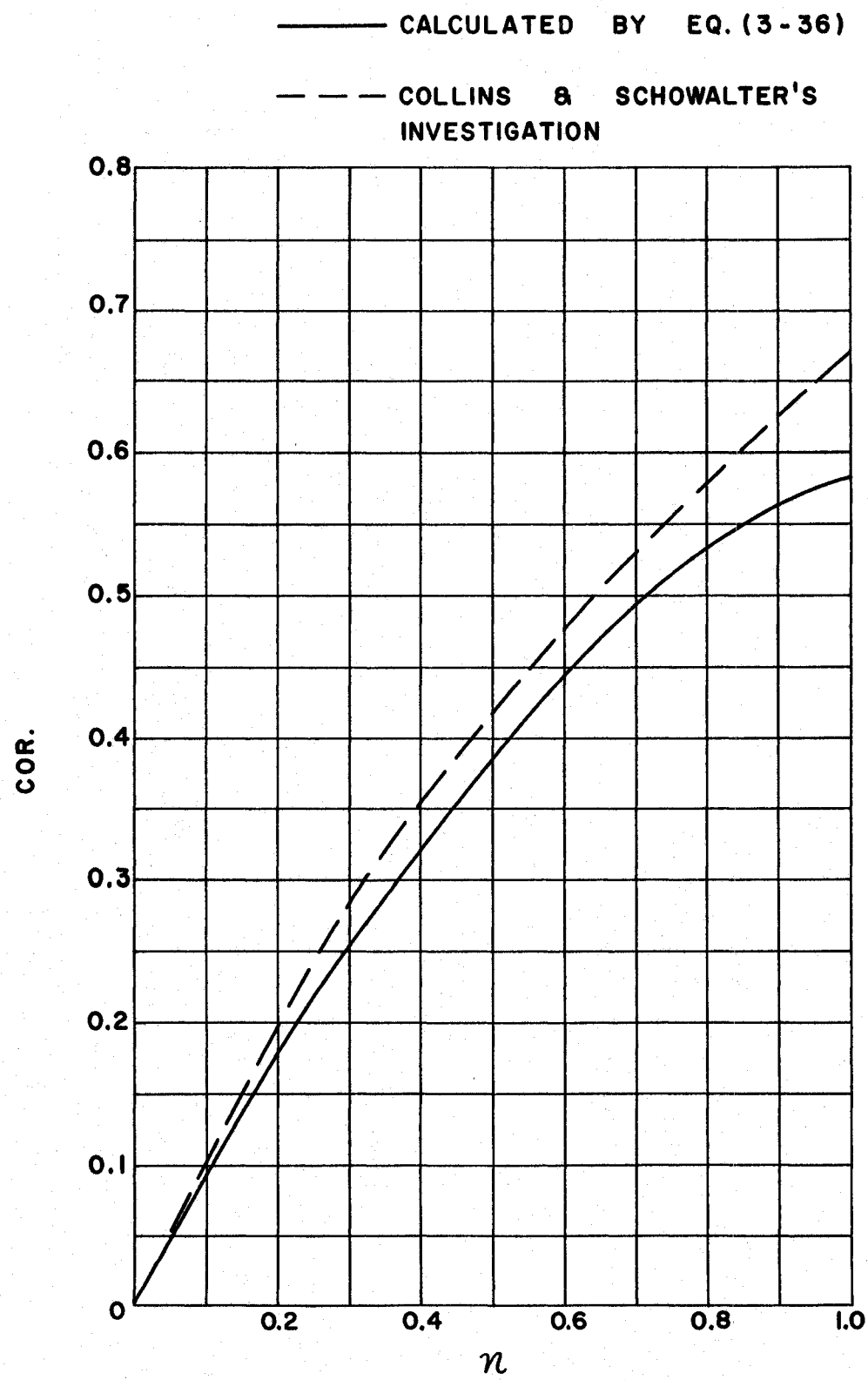

FIG. 9 ENTRY PRESSURE DROP CORRECTION "COR." VS. FLOW BEHAVIOR INDEX "n"

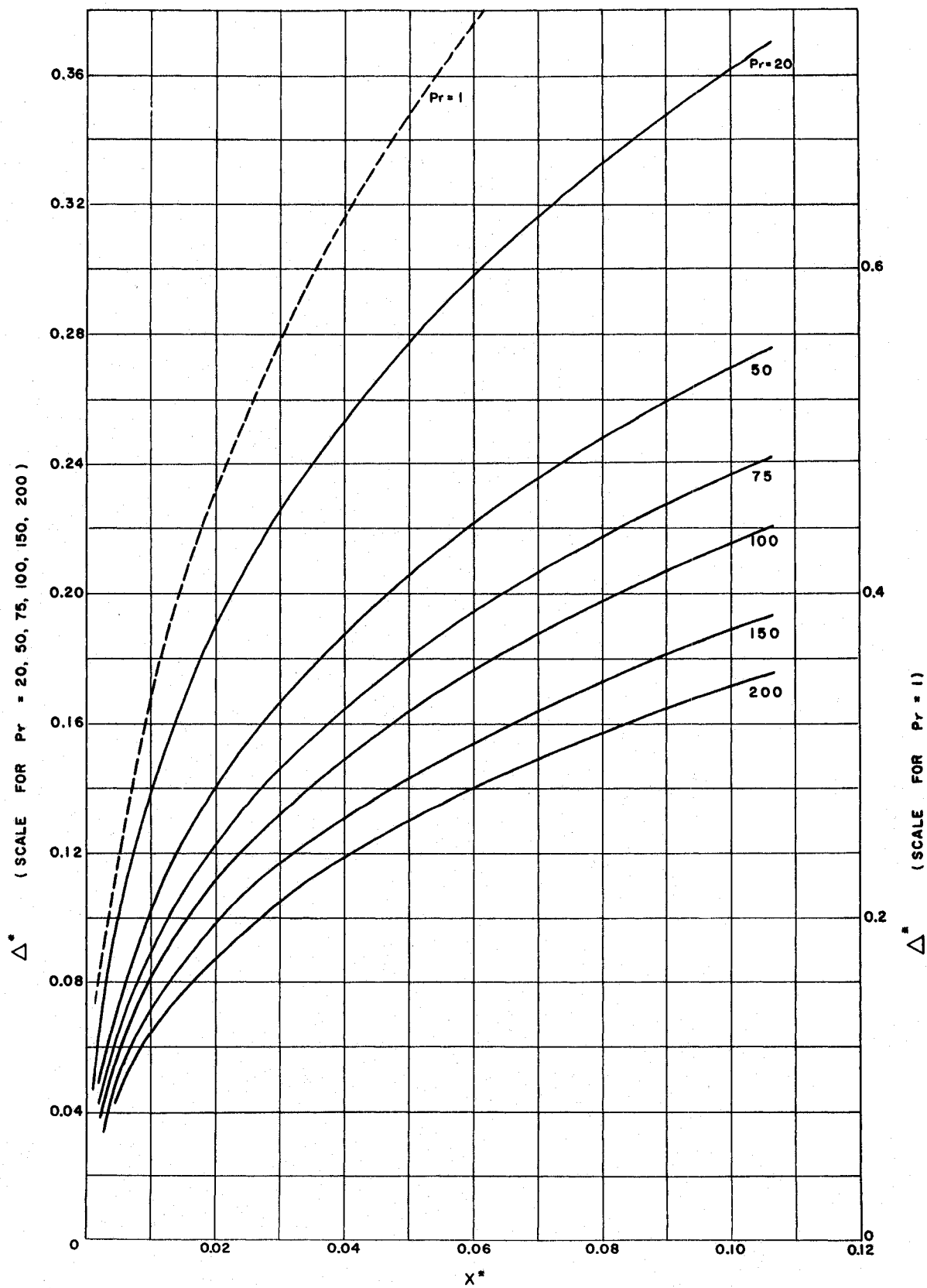

FIG. 10-A DIMENSIONLESS THERMAL BOUNDARY LAYER THICKNESS Δ^* VS. DIMENSIONLESS DISTANCE X^* FOR $n = 3/4$

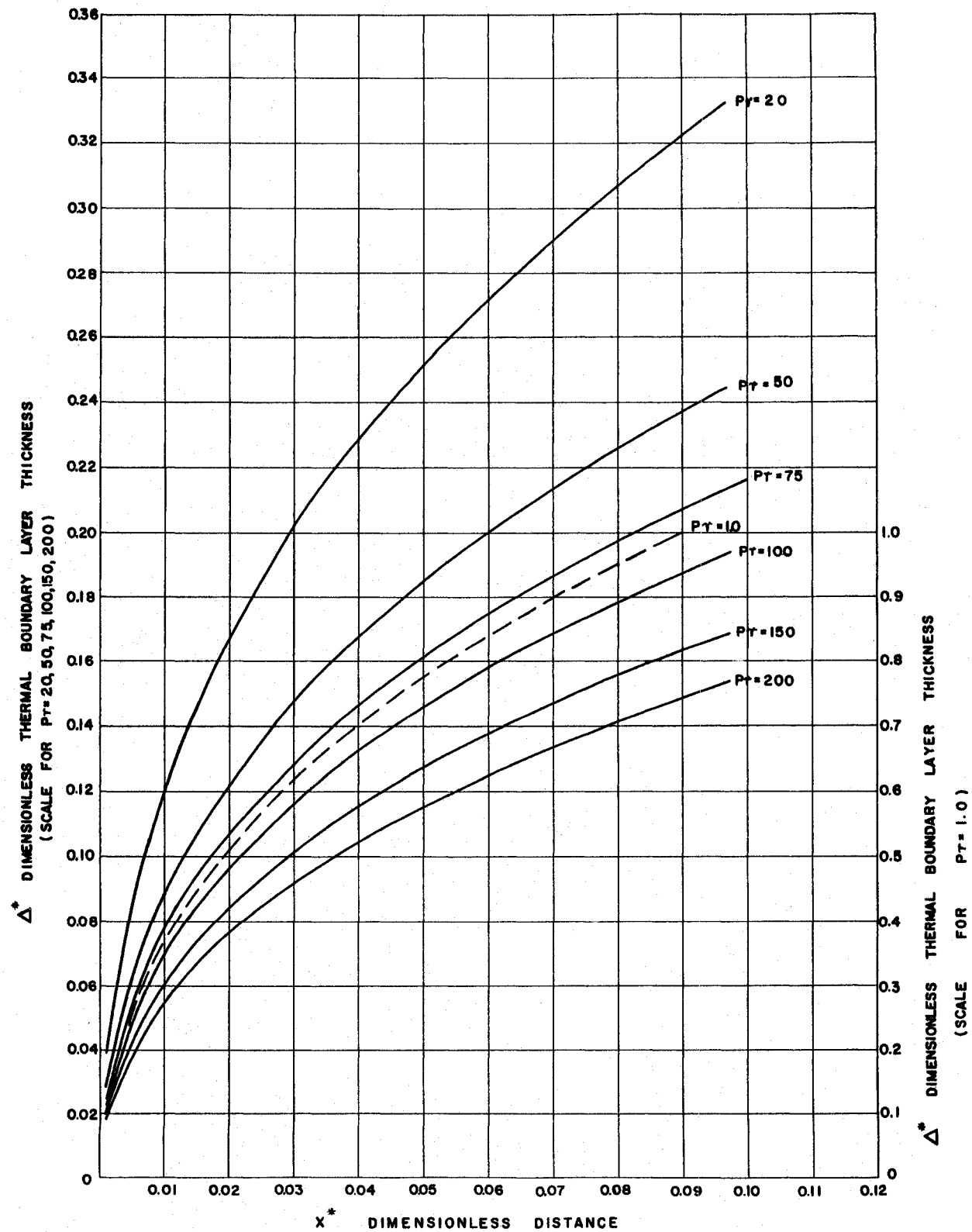

FIG. 10-B DIMENSIONLESS THERMAL BOUNDARY LAYER THICKNESS Δ^* VS. DIMENSIONLESS DISTANCE X^* FOR $n = 1/2$

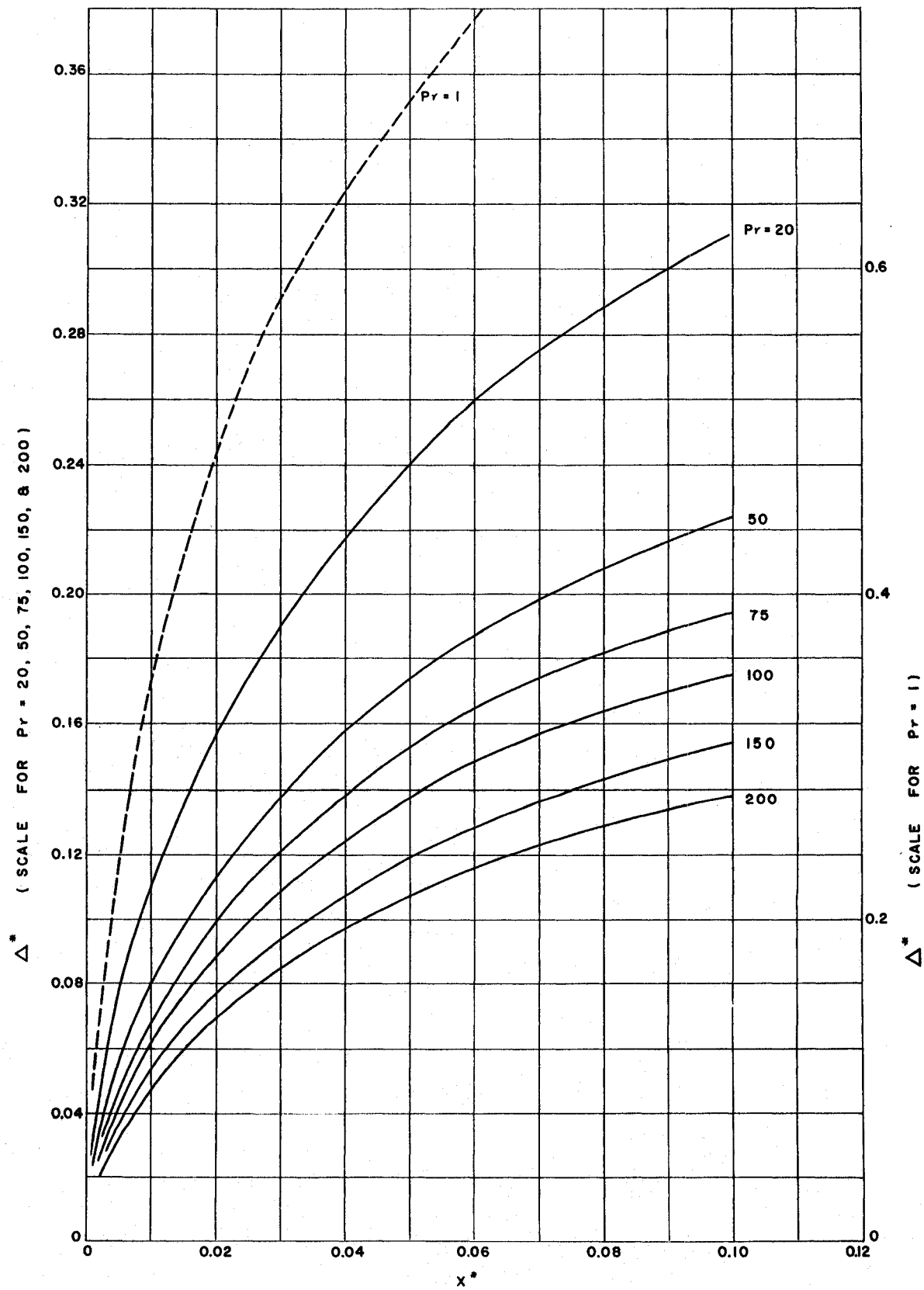

FIG. 10-C DIMENSIONLESS THERMAL BOUNDARY LAYER THICKNESS Δ^* VS. DIMENSIONLESS DISTANCE X^* FOR $n = 1/4$

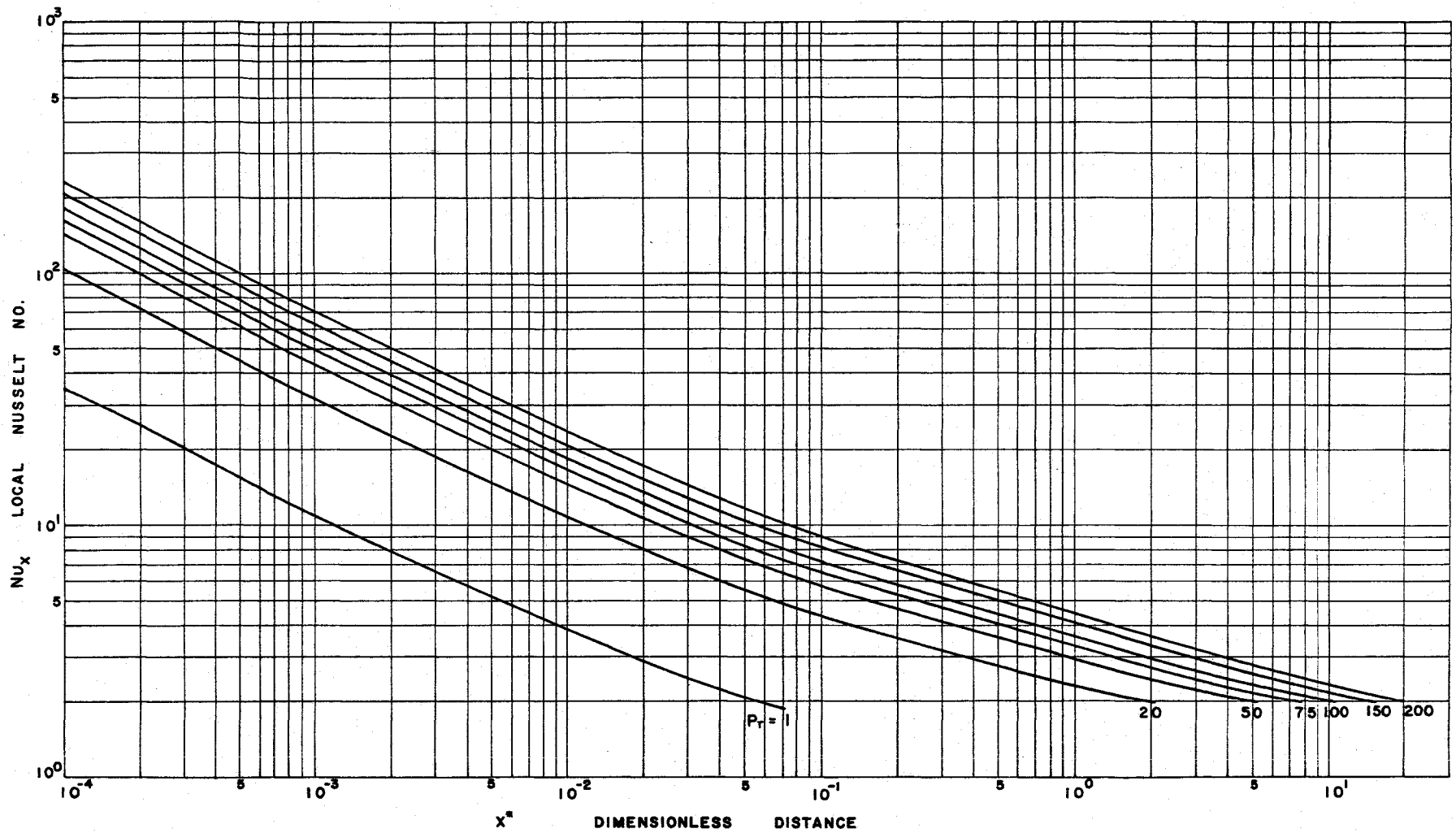

FIG. 11-A LOCAL NUSSELT NO. Nu_x VS. DIMENSIONLESS DISTANCE X^* FOR $n = 3/4$

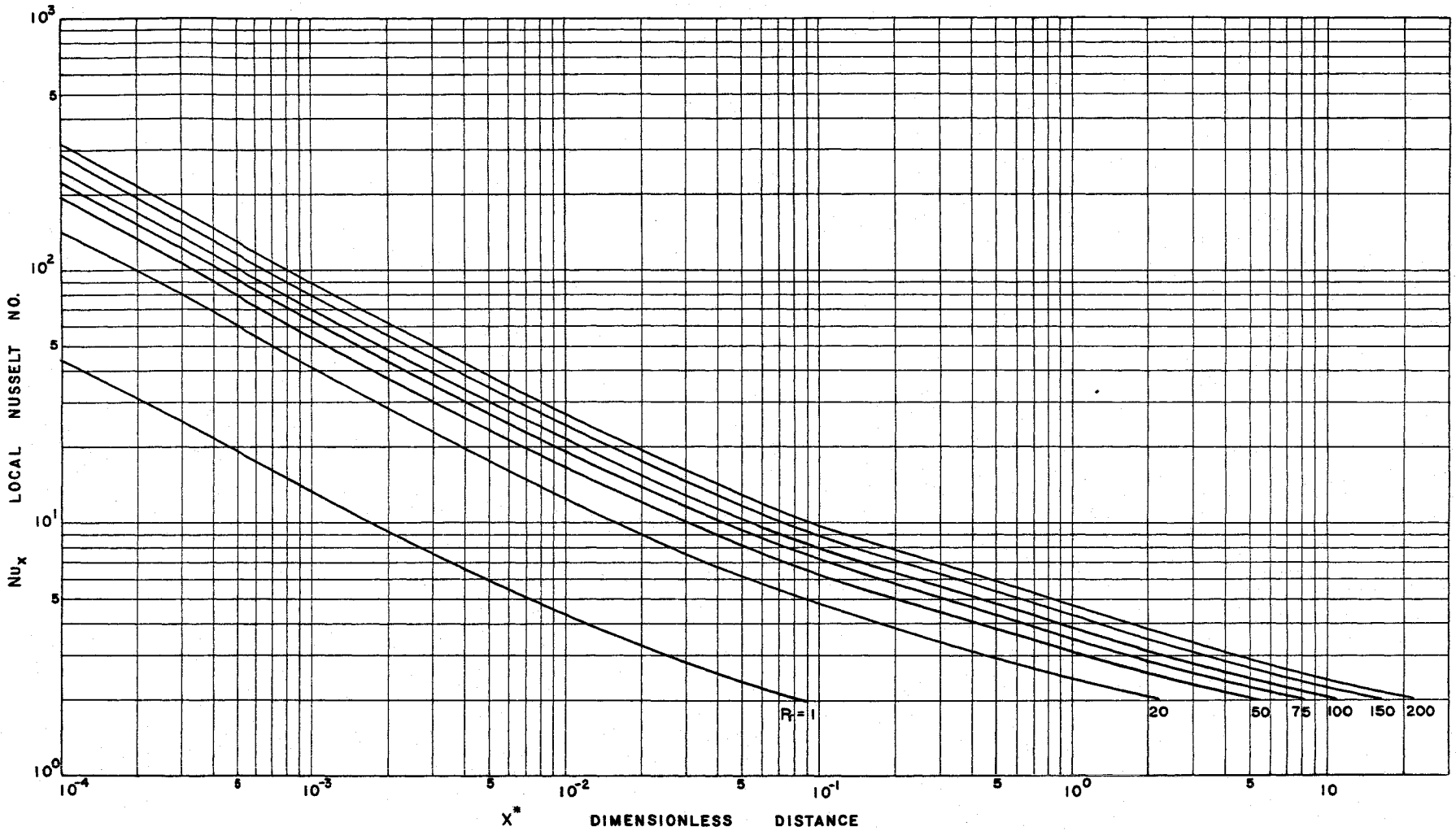

FIG. 11-B LOCAL NUSSELT NO. Nu_x VS. DIMENSIONLSS DISTANCE X^* FOR $n = 1/2$

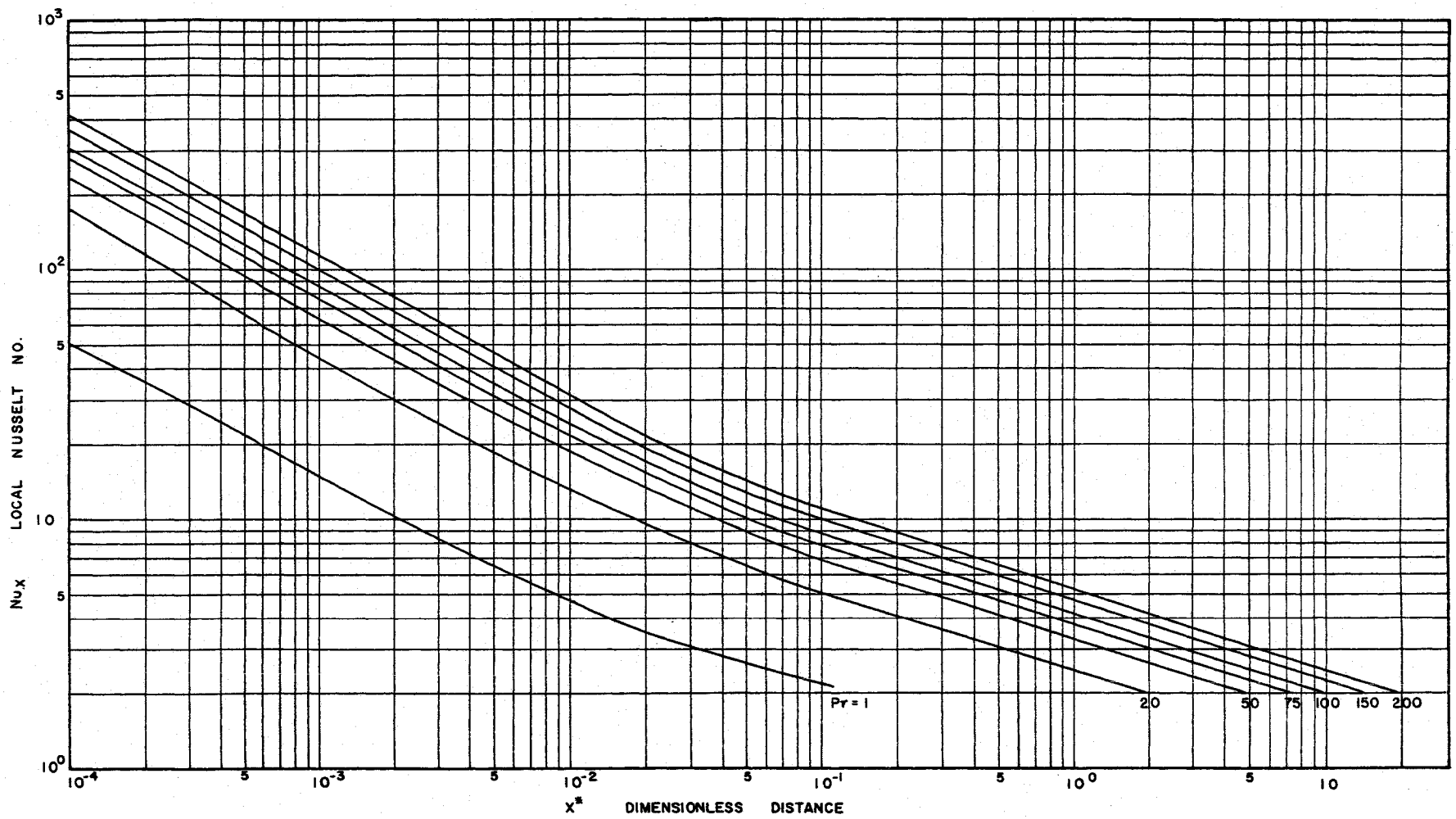

FIG. 11-C LOCAL NUSSELT NO. Nu_x VS. DIMENSIONLESS DISTANCE x^* FOR $n = 1/4$

APPENDIX G

TABLES

Table I

The Coefficients C_i for Velocity Profile

n	C_1	C_2	C_3	C_4
1.00000	2.00000	-1.00000	0	0
0.80000	2.23169	-1.27335	-0.14836	0.19002
0.75000	2.31379	-1.41205	-0.11727	0.21553
0.60000	2.65392	-2.12448	0.28718	0.18337
0.50000	3.00000	-3.00000	1.00000	0
0.40000	3.51043	-4.46358	2.39589	-0.44273
0.33333	4.00000	-6.00000	4.00000	-1.00000
0.25000	4.91056	-9.09755	7.46340	-2.27642
0.20000	5.74544	-12.14018	11.04406	-3.64931
0.11355	11.80586	-28.90242	32.38726	-12.29070

Table 2

Dimensionless Velocity (U^*) and Dimensionless Velocity Boundary Layer Thickness (δ^*) as Function of Dimensionless Distance (x^*)

For $n = 3/4$

x^*	U^*	δ^*
0.00000000	1.00	0.00000000
0.00029538	1.02	0.06535948
0.00113981	1.04	0.12820512
0.00243930	1.06	0.18867922
0.00418350	1.08	0.24691354
0.00637040	1.10	0.30303026
0.00900079	1.12	0.35714281
0.01207633	1.14	0.40935667
0.01559882	1.16	0.45977005
0.01956984	1.18	0.50847449
0.02399056	1.20	0.55555547
0.02886175	1.22	0.60109281
0.03418370	1.24	0.64516119
0.03995630	1.26	0.68783058
0.04617899	1.28	0.72916655
0.05285088	1.30	0.76923066
0.05997071	1.32	0.80808069
0.06753691	1.34	0.84577102
0.07554764	1.36	0.88235281
0.08400084	1.38	0.91787426
0.09289418	1.40	0.95238082
0.10222519	1.42	0.98591536
0.10705399	1.43	1.00233090

Table 2 (cont'd)

For $n = 1/2$

x^*	U^*	δ^*
0.00000000	1.00	0.00000000
0.00083559	1.02	0.07843138
0.00270952	1.04	0.15384614
0.00527146	1.06	0.22641507
0.00845992	1.08	0.29629625
0.01224573	1.10	0.36363632
0.01661232	1.12	0.42857137
0.02154915	1.14	0.49122800
0.02704892	1.16	0.55172406
0.03310614	1.18	0.61016939
0.03971637	1.20	0.66666657
0.04687582	1.22	0.72131137
0.05458108	1.24	0.77419343
0.06282895	1.26	0.82539670
0.07161637	1.28	0.87499986
0.08094034	1.30	0.92307679
0.09853935	1.335	1.00374520

Table 2 (cont'd)

For $n = 1/4$

x^*	U^*	δ^*
0.00000000	1.00	0.00000000
0.00257890	1.02	0.11764472
0.00698142	1.04	0.23076460
0.01231706	1.06	0.33961581
0.01846890	1.08	0.44443549
0.02538204	1.10	0.54544356
0.03302495	1.12	0.64284420
0.04137727	1.14	0.73682726
0.05042480	1.16	0.82756954
0.06015701	1.18	0.91523579
0.07056568	1.20	0.99997985
0.07327274	1.205	1.02072630

Table 3

Dimensionless Thermal Boundary Layer Thickness (Δ^*) as Function of Dimensionless Distance (x^*) and Prandtl Number (Pr)

Δ^* For $n = 3/4$

x^* \ Pr	1	20	50	75	100	150	200
0.0001	0.0430	0.0145	0.0105	0.0092	0.0083	0.0072	0.0065
0.0002	0.0615	0.0206	0.0150	0.0128	0.0120	0.0102	0.0094
0.0004	0.0872	0.0295	0.0215	0.0185	0.0170	0.0148	0.0134
0.0006	0.1070	0.0360	0.0268	0.0230	0.0210	0.0183	0.0164
0.0008	0.126	0.0420	0.0310	0.0271	0.0243	0.0212	0.0190
0.0010	0.142	0.0470	0.0347	0.0304	0.0273	0.0236	0.0214
0.0020	0.200	0.0660	0.0490	0.0425	0.0385	0.0335	0.0300
0.0040	0.275	0.0920	0.0675	0.0580	0.0530	0.0471	0.0425
0.0060	0.330	0.110	0.0800	0.0700	0.0640	0.0570	0.0512
0.0080	0.375	0.125	0.0920	0.0810	0.0730	0.0660	0.0580
0.0100	0.420	0.139	0.103	0.0890	0.0815	0.0710	0.0635
0.0200	0.580	0.190	0.141	0.123	0.111	0.0980	0.0870
0.0400	0.785	0.253	0.187	0.165	0.149	0.131	0.119
0.0600	0.930	0.298	0.222	0.194	0.176	0.154	0.140
0.0715	1.000	-	-	-	-	-	-
0.0800		0.333	0.248	0.218	0.198	0.173	0.157
0.1000		0.362	0.270	0.237	0.215	0.188	0.172
0.2000		0.447	0.327	0.286	0.260	0.227	0.216
0.4000		0.556	0.407	0.354	0.322	0.280	0.253
0.6000		0.638	0.465	0.404	0.365	0.318	0.287
0.8000		0.707	0.512	0.444	0.402	0.350	0.316
1.0000		0.766	0.551	0.479	0.433	0.377	0.340
2.0000		0.985	0.705	0.608	0.549	0.475	0.430

Table 3 (cont'd)

Δ^* For $n = 3/4$

x^* \ Pr	1	20	50	75	100	150	200
2.0758		1.000	-	-	-	-	-
4.0000			0.905	0.780	0.701	0.608	0.547
5.2197			1.000	-	-	-	-
6.0000				0.904	0.813	0.700	0.630
7.8440				1.000	-	-	-
8.0000					0.904	0.778	0.700
10.0000					0.984	0.846	0.760
10.7401					1.000	-	-
15.7230						1.000	-
20.0000							0.981
20.9771							1.000

Table 3 (cont'd)

Δ^* For n = 1/2

x^* \ Pr	1	20	50	75	100	150	200
0.0001	0.0345	0.0105	0.0077	0.0067	0.0060	0.0053	0.0048
0.0002	0.0485	0.0150	0.0113	0.0098	0.0088	0.0076	0.0069
0.0004	0.0708	0.0218	0.0164	0.0143	0.0128	0.0112	0.0100
0.0006	0.0870	0.0273	0.0205	0.0179	0.0162	0.0141	0.0124
0.0008	0.103	0.0323	0.0242	0.0211	0.0192	0.0166	0.0146
0.0010	0.116	0.0365	0.0275	0.0240	0.0216	0.0187	0.0167
0.0020	0.168	0.0540	0.0403	0.0346	0.0313	0.0272	0.0242
0.0040	0.240	0.0770	0.0576	0.0492	0.0443	0.0385	0.0345
0.0060	0.294	0.0940	0.0702	0.0600	0.0540	0.0473	0.0426
0.0080	0.335	0.1070	0.0806	0.0693	0.0615	0.0550	0.0494
0.0100	0.372	0.1220	0.0890	0.0776	0.0702	0.0610	0.0554
0.0200	0.508	0.1665	0.1217	0.1060	0.0965	0.0847	0.0754
0.0400	0.702	0.229	0.168	0.146	0.133	0.116	0.105
0.0600	0.840	0.272	0.200	0.174	0.158	0.138	0.125
0.0800	0.955	0.307	0.226	0.198	0.179	0.156	0.142
0.0900	1.000	-	-	-	-	-	-
0.1000		0.337	0.248	0.216	0.196	0.170	0.156
0.2000		0.410	0.305	0.265	0.240	0.208	0.189
0.4000		0.527	0.382	0.333	0.301	0.261	0.237
0.6000		0.612	0.440	0.382	0.345	0.300	0.271
0.8000		0.680	0.488	0.422	0.381	0.330	0.299
1.0000		0.740	0.529	0.456	0.412	0.356	0.323
2.0000		0.964	0.681	0.586	0.526	0.454	0.411
2.1892		1.000	-	-	-	-	-
4.0000			0.884	0.758	0.680	0.585	0.526

Table 3 (cont'd)

Δ^* For n = 1/2

x^* \ Pr	1	20	50	75	100	150	200
5.4658			1.000	-	-	-	-
6.0000				0.884	0.790	0.680	0.611
8.0000				0.991	0.884	0.758	0.679
8.2064				1.000	-	-	-
10.0000					0.964	0.824	0.739
10.9480					1.000	-	-
16.4306						1.000	-
20.0000							0.963
21.9144							1.000

Table 3 (cont'd)

Δ^* For n = 1/4

x^* \ Pr	1	20	50	75	100	150	200
0.0001	0.0300	0.00860	0.00644	0.00570	0.00492	0.00415	0.00360
0.0002	0.0417	0.0130	0.00960	0.00840	0.00715	0.00610	0.00528
0.0004	0.0625	0.0198	0.0142	0.0119	0.0104	0.00900	0.00780
0.0006	0.0782	0.0252	0.0177	0.0148	0.0130	0.0113	0.00975
0.0008	0.0920	0.0300	0.0208	0.0174	0.0153	0.0132	0.0115
0.0010	0.104	0.0380	0.0236	0.0197	0.0173	0.0150	0.0131
0.0020	0.155	0.0510	0.0355	0.0295	0.0262	0.0226	0.0202
0.0040	0.217	0.0730	0.0508	0.0430	0.0384	0.0330	0.0288
0.0060	0.265	0.0884	0.0622	0.0533	0.0474	0.0407	0.0356
0.0080	0.305	0.101	0.0707	0.0612	0.0548	0.0470	0.0416
0.0100	0.344	0.111	0.0790	0.0684	0.0612	0.0527	0.0475
0.0200	0.490	0.157	0.113	0.0990	0.0885	0.0768	0.0700
0.0400	0.646	0.217	0.158	0.137	0.124	0.108	0.0975
0.0600	0.742	0.260	0.188	0.164	0.149	0.130	0.118
0.0800	0.835	0.287	0.206	0.179	0.162	0.139	0.128
0.1000	0.950	0.310	0.223	0.194	0.174	0.150	0.137
0.1103	1.000	–	–	–	–	–	–
0.2000		0.392	0.278	0.243	0.220	0.188	0.171
0.4000		0.505	0.356	0.306	0.275	0.237	0.214
0.6000		0.593	0.413	0.354	0.318	0.274	0.247
0.8000		0.669	0.461	0.394	0.353	0.304	0.274
1.0000		0.735	0.502	0.428	0.383	0.331	0.296
1.9416		1.000	–	–	–	–	–
2.0000			0.662	0.562	0.501	0.417	0.383
4.0000			0.907	0.752	0.666	0.561	0.199
4.8732			1.000	–	–	–	–
6.0000				0.910	0.795	0.663	0.587
7.3172				1.000	–	–	–
8.0000					0.906	0.751	0.662
9.7624					1.000	–	–
10.0000						0.830	0.730
14.6530						1.000	–
19.5443							1.000

Table 4

The Local Nusselt Number (Nu_x) as Function of Dimensionless Distance (x^*) and Prandtl Number (Pr)

For $n = 3/4$

x^* \ Pr	1	20	50	75	100	150	200
0.0001	35.1786	103.5662	142.9454	163.1204	180.7933	208.3952	230.8259
0.0002	24.6669	72.9290	100.0849	117.2641	125.0663	147.1190	159.6286
0.0004	17.5073	50.9567	69.8494	81.1548	88.3005	101.4088	111.9929
0.0006	14.2791	41.7749	56.0496	65.2893	71.5885	82.0234	91.5155
0.0008	12.1580	35.8208	48.4659	55.6265	61.7922	70.8104	78.9991
0.0010	10.8129	32.0210	43.3058	49.1125	55.0081	63.6150	70.1446
0.0020	7.7463	22.8327	30.6894	35.3627	40.5843	44.8308	50.0654
0.0040	5.7074	16.4106	22.3009	25.9328	28.3654	31.9695	35.3444
0.0060	4.8064	13.7456	18.8317	21.5004	23.5021	26.3708	29.4630
0.0080	4.2678	12.1116	16.3868	18.5904	20.6136	22.7823	25.9143
0.0100	3.8413	10.9042	14.6457	16.9247	18.4710	21.1841	23.6754
0.0200	2.8733	8.0138	10.7248	12.2711	13.5755	15.3657	17.2974
0.0400	2.2300	6.0922	8.1160	9.1728	10.1419	11.5159	12.6643
0.0600	1.9617	5.1727	6.8723	7.8999	8.6019	9.8097	10.7770
0.0715	1.8648[§]	-	-	-	-	-	-
0.0800		4.6518	6.1538	6.9720	7.6587	8.7430	9.6198
0.1000		4.2982	5.6658	6.4244	7.0635	8.0544	8.7890
0.2000		3.5489	4.7260	5.4238	5.8778	6.7034	7.1263
0.4000		2.9455	3.8628	4.3900	4.7958	5.4779	6.0382
0.6000		2.6389	3.4293	3.8891	4.2690	4.8564	5.3529
0.8000		2.4424	3.1556	3.5740	3.9078	4.4397	4.8866
1.0000		2.3083	2.9683	3.3434	3.6555	4.1454	4.5631
2.0000		1.9936	2.4457	2.7406	2.9779	3.3714	3.6812
2.0758		1.9786	-	-	-	-	-

[§] Value of Nu_x when $\Delta^* = 1$.

Table 4 (cont'd)

Nu_x For $n = 3/4$

x^* \ Pr	1	20	50	75	100	150	200
4.0000			2.0960	2.2806	2.4593	2.7407	2.9892
5.2197			1.9933	-	-	-	-
6.0000				2.0847	2.2221	2.4637	2.6692
7.8440				1.9808	-	-	-
8.0000					2.0850	2.2877	2.4645
10.0000					1.9951	2.1672	2.3247
10.4701					1.9836	-	-
15.7230						1.9837	-
20.0000							2.0017
20.9771							1.9837

Table 4 (cont'd)

Nu_x For $n = 1/2$

x^* \ Pr	1	20	50	75	100	150	200
0.0001	43.9556	143.0781	196.2431	224.0241	250.1322	285.8296	315.8948
0.0002	31.3800	100.2135	132.8834	153.1960	170.5786	169.4445	217.8071
0.0004	21.6029	68.9996	91.6019	105.0219	117.3048	134.2712	150.8509
0.0006	17.6487	55.1406	73.3054	83.9202	92.7043	106.4816	121.0610
0.0008	14.9552	46.6286	62.1150	71.2081	78.2326	90.4570	102.8303
0.0010	13.3206	41.2810	54.6738	62.6150	69.5543	80.3078	89.9082
0.0020	9.2937	27.9487	37.3410	43.4615	48.0234	55.2352	62.0665
0.0040	6.6052	19.6448	26.1730	30.5932	33.9574	39.0526	43.5584
0.0060	5.4573	16.0960	21.4954	25.1048	27.8741	31.7970	35.2898
0.0080	4.8387	14.1842	18.7367	21.7492	24.4878	27.3562	30.4419
0.0100	4.3976	12.4558	16.9804	19.4336	21.4626	24.6739	27.1528
0.0200	3.3431	9.2745	12.4530	14.2572	15.6411	17.7942	19.9745
0.0400	2.5595	6.7360	9.0797	10.3552	11.4037	13.0748	14.3670
0.0600	2.2428	5.7040	7.6339	8.7192	9.5975	10.9922	12.0646
0.0800	2.0590	5.0781	6.7750	7.7102	8.5057	9.6965	10.6793
0.0900	2.0067	–	–	–	–	–	–
0.1000		4.6425	6.1901	7.0637	7.7632	8.9204	9.7346
0.2000		3.8980	5.0895	5.8064	6.3841	7.3297	8.0445
0.4000		3.1384	4.1376	4.6843	5.1481	5.8941	6.4608
0.6000		2.7832	3.6470	4.1313	4.5349	5.1656	5.6827
0.8000		2.5723	3.3353	3.7792	4.1420	4.7280	5.1788
1.0000		2.4233	3.1166	3.5315	3.8610	4.4089	4.8255
2.0000		2.0759	2.5591	2.8648	3.1288	3.5475	3.8675
2.1892		2.0405	–	–	–	–	–
4.0000			2.2037	2.3708	2.5580	2.8698	3.1268
5.4658			2.0251	–	–	–	–
6.0000				2.1532	2.3113	2.5596	2.7110
8.0000				2.0354	2.1581	2.3727	2.5609
8.2064				2.0284	–	–	–
10.0000					2.0643	2.2535	2.4124

Table 4 (cont'd)

Nu_x For $n = 1/2$

x^* \ Pr	1	20	50	75	100	150	200
10.9480					2.0296	-	-
16.4306						2.0341	-
20.0000							2.0652
21.9144							2.0279

Table 4 (cont'd)

Nu_x For $n = 1/4$

x^* \ Pr	1	20	50	75	100	150	200
0.0001	50.5706	174.6970	233.1681	263.3440	305.0968	361.6526	416.8668
0.0002	36.5324	115.6485	156.4740	178.7746	210.0048	246.0896	284.2748
0.0004	24.5147	75.9996	105.8383	126.2425	144.2687	166.8378	192.4802
0.0006	19.6785	59.7538	84.9417	101.5361	115.5712	132.9050	154.0110
0.0008	16.7872	50.2206	72.3344	86.3856	98.2184	113.3639	130.5926
0.0010	14.8969	39.6654	63.7433	76.3164	86.8796	100.1523	114.6564
0.0020	10.1150	29.6060	42.4184	51.0049	57.4061	66.5078	74.3894
0.0040	7.3468	20.7334	29.6838	35.0297	39.1976	45.5797	52.2073
0.0060	6.0961	17.1535	24.2688	28.2838	31.7820	36.9767	42.2547
0.0080	5.3571	15.0376	21.3704	24.6501	27.5065	32.0356	36.1743
0.0100	4.7982	13.7024	19.1406	22.0690	24.6428	28.5822	31.6917
0.0200	3.5056	9.7420	13.4230	15.2839	17.0750	19.6849	21.5321
0.0400	2.8250	7.1052	9.6730	11.0815	12.2702	14.0633	15.4863
0.0600	2.5459	5.9684	8.1105	9.2535	10.1927	11.6489	12.8137
0.0800	2.3766	5.4379	7.4265	8.5242	9.3932	10.9111	11.8272
0.1000	2.1859	5.0771	6.7751	7.8018	8.7360	10.1250	11.0930
0.1103	2.1237	–	–	–	–	–	–
0.2000		4.0926	5.6000	6.3507	6.9824	8.1263	8.9067
0.4000		3.2392	4.4595	5.1192	5.6466	6.5078	7.1733
0.6000		2.8919	3.9083	4.4815	4.9423	5.6744	6.2562
0.8000		2.6348	3.5538	4.0724	4.4942	5.1512	5.6731
1.0000		2.4600	3.3084	3.7883	4.1783	4.7624	5.2802
1.9416		2.0036	–	–	–	–	–
2.0000			2.6127	3.0148	3.3128	3.8866	4.1756
4.0000			2.1294	2.4176	2.6406	3.0195	3.3239
4.8732			2.0033	–	–	–	–
6.0000				2.1212	2.3236	2.6511	2.9143
7.3172				2.0013	–	–	–
8.0000					2.1314	2.4204	2.6107
9.7624					2.0027	–	–
10.0000						2.2593	2.4716
14.6530						2.0034	–
19.5443							2.0036

Table 5

Sample Computer Results of Integration of Equations (4-15) and (4-16) by Runge-Kutta Method

For $n = 1/4$ & $Pr = 100$

	Δ^*	U^*	δ^* 10^{-2}	$k_v/2$ & k 10^{-2}
Eq. (4-15) i.e. (D-1)	0.00010	1.0000071	0.0042925611	0.00081464648
	0.00020	1.0000153	0.0091773805	0.0012072320
	0.00020	1.0000192	0.011533191	0.0011617075
	0.00030	1.0000304	0.018229595	0.0014393288
				k = 0.0023306181
	0.00030	1.0000305	0.018274297	0.0014388085
	0.00040	1.0000448	0.026904047	0.0016466046
	0.00040	1.0000469	0.028151268	0.0016368211
	0.00050	1.0000632	0.037912014	0.0018125036
				k = 0.0032727211
	0.00050	1.0000632	0.037907543	0.0045313122
	0.00075	1.0001085	0.065088773	0.0054095627
	0.00075	1.0001173	0.070356938	0.0053711390
	0.00100	1.0001706	0.10234366	0.0042930455
				k = 0.010128590
Eq. (4-16) i.e. (D-3)	0.00100	1.0001645	0.098660193	0.0060845330
	0.00125	1.0002253	0.13515291	0.0049369985
	0.00125	1.0002138	0.12826875	0.0046036933
	0.00150	1.0002565	0.15387870	0.0048344087
				k = 0.010000108
	0.00150	1.0002645	0.15863279	0.0050582373
	0.00175	1.0003150	0.18896329	0.0054283667
	0.00175	1.0003187	0.19118053	0.0055146731
	0.00200	1.0003748	0.22476312	0.0059285411
				k = 0.010957619

Table 5 (cont'd)

For $n = 1/4$ & $Pr = 100$

	Δ^*	U^*	δ^* 10^{-2}	$k_v/2$ & k 10^{-2}
Eq. (4-16) i.e. (D-3)	0.00200	1.0003740	0.22433398	0.0059143098
	0.00225	1.0004332	0.25978960	0.0063219337
	0.00225	1.0004373	0.26223258	0.0063912083
	0.00250	1.0005019	0.30095818	0.0068128806
				k = 0.012717825
	.	.	.	.
	.	.	.	.
	.	.	.	.
	.	.	.	.
				.
	0.14000	1.1639869	84.528050	1.7159599
	0.15000	1.1811466	92.016551	1.7855563
	0.15000	1.1818425	92.315683	1.7849031
	0.16000	1.1996850	99.866056	1.8646692
				k = 3.5707100
	0.16000	1.1996940	99.869825	1.8552415
	0.17000	1.2182465	107.48596	1.9266213
	0.17000	1.2189603	107.77435	1.9257606
	0.18000	1.2382093	115.42616	1.9983201
				k = 3.8527751

VITA AUCTORIS

1939	Born in Macau, China, on May 7, 1939.
1950	Finished public school at Ling Ying Primary School, Hong Kong, in July.
1956	Graduated from St. Paul's Co-educational College, Hong Kong, with Hong Kong Government School Leaving Certificate, in June.
1961	Received the Degree of Bachelor of Applied Science in Mechanical Engineering from Assumption University of Windsor, Windsor, Ontario, in June.
1962	Currently a candidate for the Degree of Master of Applied Science in a combined programme of Chemical and Mechanical Engineering at Assumption University of Windsor.